Coordination Chemistry Reviews 531 (2025) 216479

Contents lists available at ScienceDirect

Coordination Chemistry Reviews

journal homepage: www.elsevier.com/locate/ccr

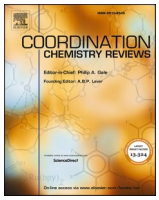

An equal terms comparison of the proficiency of artificial phosphodiesterases by using simple models of RNA or DNA as benchmarks–the takeaway to design next generation supramolecular catalysts

Alessandro Casnati [a], Riccardo Salvio [b,c,*]

[a] Dipartimento di Scienze Chimiche, Della Vita e Della Sostenibilità Ambientale, Università degli Studi di Parma, Parco Area delle Scienze, 17/A, 43124 Parma, Italy
[b] Dipartimento di Scienze e Tecnologie Chimiche, Università "Tor Vergata", Via della Ricerca Scientifica, 1, 00133 Roma, Italy
[c] ISB – CNR Sezione Meccanismi di Reazione, Università La Sapienza, 00185 Roma, Italy

ARTICLE INFO

Keywords:
Supramolecular catalysis
Kinetic analysis
Phosphodiester hydrolysis
Enzyme mimics
Artificial nucleases

ABSTRACT

This comprehensive review aims at identifying the structural features and general rules governing the design of enzyme mimics and supramolecular catalysts having the ability to hydrolytically cleave the phosphodiester bonds. Rate and binding constants of the artificial phosphodiesterases so far proposed and tested by using the model compounds, bis (*p*-nitrophenyl) phosphate (BNPP) and 2-hydroxypropyl *p*-nitrophenyl phosphate (HPNP) as widely recognized model substrates have been collected, elaborated and compared. These substrates have been extensively used over time to evaluate the performance of artificial phosphodiesterases, providing consistent and unique bases for comparing different catalysts. Notably, no other substrates have been tested as extensively and over such a prolonged period. A wide variety of supramolecular phosphodiesterases have been considered, comprising metal-free- and metallocatalysts, acyclic, macrocyclic or even nanostructured ones. The scope and limits of the use of Effective Molarity to evaluate the enhanced reactivity of some of these supramolecular catalysts are also discussed. The information collected allows to give the reader a take-home message for the design of next generation artificial phosphodiesterases.

1. Introduction

Phosphodiester bond represents the linker of nucleic acids, serving as a tool to keep the nucleotides together and, at the same time, put them apart at the proper moment [1]. Its reluctance to undergo hydrolysis [2] makes it ideal for preserving biochemical information. However, the cleavage of phosphodiester bonds is a pivotal chemical transformation in living organisms and, consequently, there are a relevant number of enzymes able to catalyze their fast hydrolysis in water [3–7]. The accelerations of the reaction rates experienced in the presence of these enzymes (e.g. kinases, phosphatases, ATPases) are impressive in a large number of cases [8–11]. Indeed, *staphylococcal nuclease* shows an acceleration over the spontaneous reaction as high as 10^{17} [9].

Inspired by the natural enzymes, a large number of research groups have designed, synthesized and tested numerous enzyme mimics able to cleave fragments of RNA, DNA in an effective and selective fashion [12–25], with a great interest for a large variety of research areas including the antisense therapy [26,27] and other biomedical applications [28–31]. Nevertheless, the cleavage rate enhancements experienced by nucleic acids in the presence of these enzyme mimics are lower than those observed in the presence of natural enzymes. As a result of that, the reaction time range needed for a reliable measurement tends to be too wide, especially in the case of deoxyribonucleic acids, intrinsically much less reactive than their ribonucleic counterparts [2]. In addition to that, the detection and the quantification of the hydrolysis products over time, essential for the determination of the reaction rates, is not straightforward, especially at sub-millimolar concentration. In order to overcome these problems, the performances of the catalysts were tested, in a very large number of cases, on activated model compounds, producing *p*-nitrophenol as cleavage product, whose release can be easily followed by UV–Vis spectrophotometry or other techniques [32–34]. The two model substrates, extensively employed to test

* Corresponding author at: Dipartimento di Scienze e Tecnologie Chimiche, Università "Tor Vergata", Via della Ricerca Scientifica, 1, 00133 Roma, Italy.
E-mail address: riccardo.salvio@uniroma2.it (R. Salvio).

https://doi.org/10.1016/j.ccr.2025.216479
Received 21 October 2024; Received in revised form 24 December 2024; Accepted 20 January 2025

enzyme mimics, are the bis(*p*-nitrophenyl) *phosphate* (BNPP) and the 2-hydroxypropyl *p*-nitrophenyl phosphate (HPNP), see Scheme *1*, model compounds of DNA and RNA respectively. Their synthesis was reported for the first time between the '50s and '60s [35,36] but they were not used with this purpose since the beginnings of '90s [37–39]. While the BNPP cleavage requires the assistance of an external nucleophile to undergo hydrolytic cleavage (Eq. 1, Scheme 1), HPNP features an hydroxyl unit on 2' position on the propyl chain that enables an intramolecular nucleophilic attack onto the phosphorous atom, affording a five-membered cyclic species, Eq. 2. Its structure mimics the RNA structural motif consisting in a hydroxyl group in 2' position on the ribose ring.

These two model compounds turned out to be fully appropriate to test, in a preliminary screening, the efficiency of the supramolecular systems as, in a number of cases, they were also tested on di(ribo)nucleosides, oligo(ribo)nucleosides, and plasmids exhibiting accelerations much higher than those experienced in the presence of the models [40–44], aside from a few exceptions [45]. Indeed, if a substrate is already partially activated, such in the case of the aforementioned substrates, it is expected to benefit less from the activation of a catalyst, with an underestimation of the acceleration factors. This evidence can be framed within the Reactivity-Selectivity Principle (RSP) [46]. Even though such a rule is not considered general and theoretically well-grounded anymore [47], in this instance it appears to be applicable as the use of HPNP and BNPP effectively provides an initiatory selection of potential artificial (ribo)nucleases.

These two phosphodiesters, because of their availability, reactivity in the right time interval, and the ease of quantification of the reaction product, have been used as substrates for a large number of enzyme mimics in a time period that spans three decades. Indeed, this has enabled the collection of consistent, homogeneous kinetic data, allowing for a direct quantitative comparison of all the catalysts on equal terms. In this review article we have summarized the strategies used to design the supramolecular catalysts and their features with a list of selected examples. This selection was based on the catalyst efficiency, on its representativeness among the class of artificial phosphodiesterases and on the availability of quantitative data for the hydrolysis of BNPP and HPNP. All the relevant rate constants and binding constants were extracted from these literature contributions, reported in the tables below, compared and critically commented. In some cases, the data were provided by the authors with different notations. In others, the values in the tables were not directly reported by the authors but obtained from other data available in the literature. In addition, the issue of the dependence of the catalytic rate and binding constants on the structural identity of the catalytic platform is tackled and discussed in terms of effective molarity. This parameter that can be taken, in a limited number of cases, as a quantitative measurement that summarizes the performance of an enzyme mimic. All the examples discussed are not reported in chronological order but following an increasing complexity of the supramolecular scaffolds and catalytic efficiency.

Although data collected on HPNP or BNPP models cannot be directly extrapolated to the cleavage of natural nucleic acids, the takeaway messages that can be drawn from this analysis of the literature for the design of artificial phosphodiesterases are:

i) metal ion-based catalysts are usually superior to metal-free catalysts
ii) in both metallocatalysts and metal-free catalysts, a proper selection of the ligand/metal ion couple and/or of the active units is necessary
iii) the simultaneous presence of multiple active units (containing or not containing metal ions) on a molecular platform (multifunctional catalysts) are generally superior to monofunctional catalysts only when the distance and the orientation between active units are properly tuned
iv) in multifunctional catalysts, the choice of the platform is crucial since it should better offer a certain flexibility and adaptability of the distance between active units to achieve remarkable cooperative effects
v) the use of nanostructured materials affords adaptable catalytic sites that can act cooperatively enhancing the overall catalytic performance.

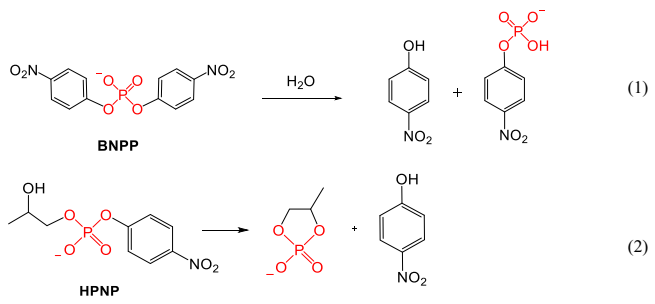

Scheme 1. Cleavage reactions for the model substrate BNPP (1) and HPNP (2).

2. Kinetic analysis and notations

For the supramolecular catalysts considered in the present paper, the cleavage mechanism consists in a pre-equilibrium affording the complex *CS* where the two molecules interact through hydrogen bonding, electrostatic and Lewis acid-base interactions (Eq. (3)) [12,14,46,48,49]. Unlike natural enzyme, for these artificial catalysts the k_{cat} value is always negligible compared to k_{-1}, therefore in the kinetic treatment is always a good approximation to take in consideration the binding constant K_b defined in Eq. (4), typically in the order of 10^1–10^3 M^{-1}. In a few papers, the authors consider the dissociation constants K_M, called Michaelis-Menten constant, instead of the binding constant K_b as defined in (4). These values, for the sake of homogeneity, were easily converted through the following equivalence: $K_b = 1/K_M$. The spontaneous cleavage [50,51] (background reaction) of the substrates k_{bg} is negligible in all the cases reported unless at extreme pH values where it might become comparable with the catalyzed reaction, especially in the case of HPNP [50,52,53]. This latter substrate undergoes both acid and basic hydrolysis [50]. In addition, there is also a contribution of the mere solvent at pH around the neutrality, therefore the plot of log k_{bg} versus pH shows a U-shaped profile in water. The value of the first-order rate constant for the spontaneous cleavage of HPNP in water is given by the following expression: $k_{bg} = k_{OH}[OH^-] + k_{sp} + k_H[H^+]$ with the values of best fit parameters determined by experimental kinetic experiments (see Ref. [50] and note *c* in Table 1). Even though the spontaneous cleavage is negligible in the presence of all the catalysts considered in the present study, the background contribution is important to determine the acceleration ratio ($k_{rel} = k_{obs}/k_{bg}$) provided by the catalyst, that is an essential parameter to evaluate its performance.

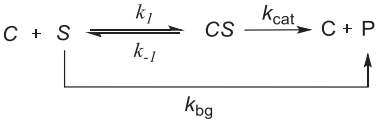

(3)

$$K_b = \frac{k_1}{k_{-1}} \tag{4}$$

$$\frac{d[CS]}{dt} = k_1[C][S] - k_{cat}[CS] - k_{-1}[CS] = 0 \tag{5}$$

Considering the mechanism illustrated in Eq. (3), if the steady state approximation is applied to the concentration of *CS*, i.e. Eq. (5), the general expression of the rate constant k_{obs} is given by Eq. (6), and the reaction rate by Eq. (7), where [C] is the free catalyst concentration and

Table 1
Kinetic Data for the Transesterification of HPNP promoted by the listed catalysts [a].

Entry	Catalyst	k_{obs} (s^{-1}) [b]	$k_{rel} = k_{obs}/k_{bg}$ [c]	k_2 (s^{-1} M^{-1})[d]	K_b (M^{-1})[e]	k_{cat} (s^{-1})[e]	Conditions	Refs. [f]
1	**1**-Cu^{II}	1.9×10^{-5}	690	1.9×10^{-2}	–	–	pH = 7.0 [g]	[77]
2	**2**-Cu^{II}	1.3×10^{-5}	110	1.3×10^{-2}	–	–	pH = 8.0	[77]
3	**3**-Cu^{II}	8.1×10^{-5}	2900	8.1×10^{-2}	–	–	pH = 7.0	[77]
4	**4**-Cu^{II}	4.1×10^{-5}	1500	4.1×10^{-2}	–	–	pH = 7.0	[78]
5	TACD-Zn	8.6×10^{-6}	2300	4.3×10^{-2}	–	–	pH = 7.0 AcCN/H_2O 50 % [h]	[81]
6	TACD -Cu	3.3×10^{-6}	75	1.6×10^{-2}	$< 10^2$	–	pH = 7.0 AcCN/H_2O 50 % [h]	[81]
7	TACN-Zn^{II}	7.0×10^{-6}	18	7.0×10^{-3}	–	–	pH = 7.2, 40 °C	[82,83]
8	TACN-Cu^{II}	1.4×10^{-6}	700	2.8×10^{-3}	–	–	pH = 8.8 [i,j] DMSO/H_2O 80 %	[41]
9	TACN-Ni^{II}	8.0×10^{-7}	2.0	8.0×10^{-4}	–	–		[82]
10	BAMP-Zn^{II}	3.4×10^{-6}	180	3.4×10^{-3}	–	–	pH = 7.0, AcCN/H_2O 50 %	[84]
11	**6**-La^{III}	1.1×10^{-4}	2.0×10^4	0.65	–	–	pH = 7.4, T = 37 °C	[86]
12	**6**-Ce^{III}	1.0×10^{-4}	1.8×10^4	5.9×10^{-1}	–	–	pH = 7.4, T = 37 °C	[86]
13	**7**-La^{III}	1.2×10^{-4}	740 [r]	0.66	–	–	pH = 7.4, 37 °C	[155]
14	**8**-Cu^{II}	3.3×10^{-5}	1000	3.3×10^{-2}	–	–	pH = 7.4, 37 °C	[88]
15	**9**-Zn^{II}	2.2×10^{-5}	16	5.7×10^{-2}	–	–	pH 8.5 MeOH/water 33 %	[89]
16	**10a**-Zn^{II}	1.0×10^{-4}	10	1.2×10^{-1}	–	–	pH = 10.0	[90]
17	**10b**-Cu^{II}	1.7×10^{-4}	170	1.7×10^{-1}	–	–	pH = 9.0	[91]
18	**10b**-Zn^{II}	1.8×10^{-4}	180	1.8×10^{-1}	–	–	pH = 9.0	[91]
19	**11a**-$(Cu^{II})_2$	5.0×10^{-6}	5.0	1.1×10^{-2}	–	–	pH = 9.0	[91]
20	**11b**-$(Cu^{II})_2$	6.1×10^{-6}	6.1	1.3×10^{-2}	–	–	pH = 9.0	[91]
21	**12**-$(Cu^{II})_2$	1.0×10^{-4}	3600	0.11	130	8.7×10^{-4}	pH = 7.0	[92]
22	**13**-$(Zn^{II})_3$	5.0×10^{-5}	240	2.5	180	1.1×10^{-3}	pH = 7.2 40 °C [cat] = 20 μM	[93]
23	**14**-$(Zn^{II})_2$	1.6×10^{-6}	120	3.2×10^{-3}	–	–	pH = 7.0	[94,95]
24	**15** $Mo_7O_{24}^{6-}$	6.6×10^{-6}	–	1.6×10^{-5}	0.94	3.0×10^{-4}	pD = 5.9 T = 50.0 °C [cat] = 0.4 M	[34]
25	**5e**-Cu^{II}	1.3×10^{-5}	1000	1.3×10^{-2}	–	–	pH = 6.2 EtOH/H_2O 35 %	[97]
26	**16**-$(Cu^{II})_2$	4.2×10^{-4} [h]	3.2×10^4	0.52	2.5×10^2	2.1×10^{-3}	pH = 6.2 EtOH/H_2O 35 %	[97]
27	**17a**-$(Zn^{II})_2$	1.2×10^{-5}	1300	1.3×10^{-2}	7.5×10^2	1.9×10^{-5}	pH = 7.0 MeCN/H_2O 50 %	[97]
28	**17b**-$(Zn^{II})_2$	7.7×10^{-4}	4.0×10^4 [h i]	43	5.5×10^4	7.7×10^{-4}	pH = 7.0 MeCN/H_2O 50 %	[97]
29	**17b**-$(Zn^{II})_2$	9.4×10^{-4}	1.6×10^4 [h]	17	1.7×10^4	1.0×10^{-3}	pH = 7.4 MeCN/H_2O 50 %	[97]
30	**18**-$(Zn^{II})_2$	2.0×10^{-4}	7400	0.68	1.9×10^3	3.6×10^{-4}	pH = 6.8, MeCN/H_2O 50 %	[99]
31	**19**-$(Zn^{II})_2$	8.2×10^{-5}	4300 [k]	0.68	7.0×10^3	9.5×10^{-5}	pH = 7.0 MeCN/H_2O 50 %	[100]
32	**20**-$(Zn^{II})_3$	8.5×10^{-4}	4.5×10^4 [l]	2.9	1.2×10^3	2.4×10^{-3}	pH = 7.0 MeCN/H_2O 50 %	[84,100]
33	**21**-$(Zn^{II})_2$	1.5×10^{-4}	38	0.15	–	–	pH = 8.0	[101]
34	**21**$(Zn^{II})_2$ +β-CD	2.7×10^{-3}	690	4.5	300	1.2×10^{-2}	pH = 8.0, T = 40 °C 5.0 mM β-CD [cat] = 0.4 mM	[101]
35	**22**-$(Zn^{II})_2$	2.5×10^{-6}	12	5.0×10^{-3}	–	–	pH = 7.2 T = 40 °C	[82]
36	**22**-$(Ni^{II})_2$	1.3×10^{-6}	6	2.6×10^{-3}	–	–	pH = 7.2 T = 40 °C	[82]
37	**22**-$(Cu^{II})_2$	2.0×10^{-7}	0.5	4.0×10^{-4}			pH = 7.2 T = 40 °C	[82]
38	**23**-$(Zn^{II})_2$	2.1×10^{-5}	110	4.2×10^{-2}	2.5×10^2	1.7×10^{-4}	pH = 7.2 T = 40 °C	[82]
39	**23**-$(Ni^{II})_2$	6.0×10^{-6}	30	1.2×10^{-2}	–	–	pH = 7.2 T = 40 °C	[82]
40	**23**-$(Cu^{II})_2$	4.0×10^{-6}	20	8.0×10^{-3}	–	–	pH = 7.2 T = 40 °C	[82]
41	**24**-$(Cu^{II})_2$	1.0×10^{-5}	210	1.0×10^{-1}	2.6×10^2	3.9×10^{-4}	pH = 7.0 40 °C	[103]
42	**25a**-$(Zn^{II})_4$	1.6×10^{-4}	160 [o]	1.6×10^{-1}	–	–	pH = 7.4 40 ° C	[83]
43	**25b**-$(Zn^{II})_2$	9.4×10^{-5}	96 [o]	9.4×10^{-2}	–	–	pH = 7.4 40 ° C	[83]
44	**25c**-$(Zn^{II})_2$	8.4×10^{-5}	86 [m]	8.4×10^{-2}	–	–	pH = 7.4 40 ° C	[83]
45	**26**-$(Zn^{II})_4$	1.2×10^{-5}	1500	6.0×10^{-2}	–	–	pH = 7.0	[105]
46	**27**	6.6×10^{-6}	240	3.3×10^{-3}	–	–	pH = 7.0	[104]
47	**28a**-$(Zn^{II})_2$	6.3×10^{-6}	1700	3.2×10^{-2}	–	–	pH = 7.0 AcCN/H_2O 50 %	[81]
48	**28b**-$(Zn^{II})_2$	6.0×10^{-6}	1600	3.0×10^{-2}	–	–	pH = 7.0 AcCN/H_2O 50 %	[81]
49	**28c**-$(Zn^{II})_3$	2.1×10^{-5}	5800	1.1×10^{-1}	–	–	pH = 7.0 AcCN/H_2O 50 %	[81]
50	**28a**-$(Cu^{II})_2$	2.4×10^{-4}	5500	1.2	–	–	pH = 7.0	[81]
51	**28b**-$(Cu^{II})_2$	8.7×10^{-6}	200	4.4×10^{-2}	–	–	pH = 7.0	[81]
52	**28c**-$(Cu^{II})_3$	1.3×10^{-4}	3000	6.5×10^{-1}	500	7.6×10^{-4}	pH = 7.0	[81]
53	**29**-$(Zn^{II})_2$	2.5×10^2	6.1×10^{11} [p]	2.8×10^5	120	2.3×10^3	[s]pH = 9.8, MeOH	[106,107]
54	**30**-Gd^{III}	4.7×10^{-5}	47	4.7×10^{-2}	–	–	pH = 9.0	[111]
55	**31**-Zn^{II}	1.3×10^{-6}	37	1.3×10^{-3}	11	1.2×10^{-4}	pH = 7.6	[14,112,113]
56	**32**-Zn^{II}	2.8×10^{-4}	280	2.8×10^{-1}	–	–	pH = 9.0	[156]

(*continued on next page*)

Table 1 (*continued*)

Entry	Catalyst	k_{obs} (s^{-1}) [b]	$k_{rel} = k_{obs}/k_{bg}$ [c]	k_2 (s^{-1} M^{-1})[d]	K_b (M^{-1})[e]	k_{cat} (s^{-1})[e]	Conditions	Refs. [f]
57	**32**-Zn^{II}	1.0×10^{-4}	3700	1.0×10^{-1}	–	–	pH = 7.0	[156]
58	**33**-$(Zn^{II})_2$	8.0×10^{-5}	2900	8.6×10^{-2}	76	1.1×10^{-3}	pH = 7.5 EtOH/H_2O 8/2	[157]
59	**34**-$(Cu^{II})_2$	3.0×10^{-5}	1100	3.1×10^{-2}	120	2.8×10^{-3}	pH = 7.5	[158]
60	**35**-$(Cu^{II})_2$	2.1×10^{-3}	7.6×10^{4}	2.1	–	–	pH = 7.0	[78]
61	**36**-$(Zn^{II})_2$	1.8×10^{-3}	1.0×10^{10} [p]	18	1.8×10^{5}	1.0×10^{-4}	pH = 7.3 MeOH	[114]
62	**37**-Zn^{II}	7.0×10^{-4}	5800	7.0×10^{-1}	–	–	pH = 8.0	[115]
63	**38**	8.0×10^{-5}	510 [i,j]	4.0×10^{-2}	<50 [q]	-	pH = 10.1 DMSO/H_2O 80 % [i,j]	[53]
64	**39**	6.9×10^{-5}	290	2.3×10^{-2}	< 50 [q]	-	pH = 10.1 DMSO/H_2O 80 % [i,j] [cat] = 3 mM	[51]
65	**40**	3.4×10^{-5}	2100	6.8×10^{3}	–	-	pH = 8.7 DMSO/H_2O 80 % [i,j] [cat] = 5.0 mM	[52]
66	**41a**-Cu^{II}	1.4×10^{-5}	250	7.0×10^{-3}	–	-	pH = 7.0	[125]
67	**41b**-Cu^{II}	5.1×10^{-4}	7700	0.10	–	-	pH = 9.0 DMSO/H_2O 80 % [i,j] [cat] = 5.0 mM	[117]
68	**41b**-Zn^{II}	1.0×10^{-3}	2500 [t]	0.2	–	-	pH = 9.8 DMSO/H_2O 80 % [i,j] [cat] = 5.0 mM	[117]
69	**42a**-Zn^{II}	1.1×10^{-4}	4400	2.2×10^{-1}	< 50 [q]	-	pH = 9.9 DMSO/H_2O 80 %	[41]
70	**42a**-Cu^{II}	1.3×10^{-3}	6.5×10^{5}	2.6	–	-	pH = 8.8 DMSO/H_2O 80 % [i,j]	[41]
71	**42b**-Cu^{II}	1.8×10^{-3}	7.2×10^{5}	3.6	–	-	pH = 8.9 DMSO/H_2O 80 % [i,j]	[126]
72	**43**	5.5×10^{-6}	2200	6.3×10^{-2}	1.4×10^{2}	4.4×10^{-5}		[127]
73	**44**-$(Zn^{II})_{16}$ d_{16}	1.2×10^{-5}	2.0×10^{4} [n] 910 [o]	9.5	1.4×10^{3}	6.7×10^{-3}	pH = 7.5 40 °C AcCN/H_2O 3/7 [TACN] = 2e-5, [cat] = 1.3e-6	[128]
74	**45**-$(Zn^{II})_{32}$ D_{32}	1.3×10^{-6}	4.5×10^{4} [n] 2000 [o]	19	1.3×10^{2}	1.6×10^{-2}	pH = 7.5, 40 °C AcCN/H_2O [TACN] = 2e-5 [cat] = 6.0e-7 M	[128]
75	**46**-$(Zn^{II})_n$	2.0×10^{-4}	1.6×10^{4} [u]	4.6	3.3×10^{3}	1.4×10^{-3}	pH = 7.0,40 °C [TACN] = 20 μM	[136]
76	**47**	1.1×10^{-5}	500	0.05	–	–	pH = 10.2 DMSO/H_2O 80 % [i,j] [guanidine] = 0.2 mM	[133]
77	**48**	2.8×10^{-5}	2800 [s]	0.14	–	–	pH = 9.9 DMSO/H_2O 80 % [i,j] [guanidine] = 0.20 mM	[139]
78	**49**	2.6×10^{-4}	3100 [o]	5.7	1900	3.0×10^{-3}	pH = 7.0, 40 °C [cat] = 50 μM	[143]
79	**49b**	3.7×10^{-3}	1.8×10^{4}	39	650	6.0×10^{-2}	[cat] = 100 μM	[146]
80	**49c**	8.7×10^{-5}	930	7.8×10^{-1}	600	1.3×10^{-3}	[cat] = 120 μM pH = 7.5, 37 °C	[147]
81	NDs@**50**	9.3×10^{-5}	1300	1.3	–	–	pH = 9.0 [cat] = 69 μM	[154]

[a] solvent = water and T = 25 °C unless otherwise stated. Catalyst concentrations range from 0.1 to 2.0 mM; and HPNP initial concentration from 0.050 to 0.20 mM, unless otherwise indicated. In a few cases the concentration of active units is indicated: e.g. guanidinium, TACN, *etc*; [b] The k_{obs} values were typically measured with the initial rate method according to the following expression: $k_{obs} = v_o$/[HPNP]; experimental error for the rate constants ranges from 5 to 15 %. These values refer to the measurement at the actual catalyst concentration chosen by the authors in the experiments. Whenever the catalyst concentration was not clearly indicated by the authors this value has been extrapolated at 1.0 mM catalyst concentration. [c] The value of the first-order rate constant for the spontaneous cleavage of HPNP in water is given by the following expression: $k_{bg} = k_{OH}[OH^-] + k_{sp} + k_H[H^+]$ with the following vales of best fit parameters determined by experimental kinetic experiments: $k_{OH} = 1.0 \times 10^{-1}$ s^{-1} M^{-1}, $k_{sp} = 1.7 \times 10^{-8}$ s^{-1}, $k_H = 3.1 \times 10^{-5}$ s^{-1} M^{-1} (see Ref. [50]), see also the comment in Section 2, main text. The acceleration factor k_{obs}/k_{bg} has been calculated using k_{obs} extrapolated to 1.0 mM catalyst concentration using the reported data and Eq. (6), also for those catalysts that were tested at slightly different concentration. In the case K_b and k_{cat} were not determined, this value has been calculated by linear extrapolation of k_{obs}. The accelerations over the background reaction are reported with two significant figures. [d] This value has been calculated with the following formula: $k_2 = K_b \times k_{cat}$. For the catalysts that were not investigated in a *pesudo* Michaelis-Menten experiments, the k_2 values were approximately determined with the following equation: $k_{2=} k_{obs}/[C]_T$. [e] These values were omitted in the case no saturation kinetic experiments has been carried out by the authors and consequently no catalyst-substrate binding constant can be determined. The error limit on the binding constant can be considered in the order of ±20 %; [f] literature reference, see reference list at the bottom of the manuscript. [g] the authors reports about the formation of the a monohydroxo or dihydroxo species at higher metal concentration with the formation of dimeric species. Around 1 mM catalyst concentration the influence of this effect on the reactivity is very low [77]. [h] The spontaneous transesterification of the HPNP in this solvent mixture, i.e. AcCN/H_2O 50 % is $k_{bg} = 1.9 \times 10^{-8}$ s^{-1} (pH = 7.0) and $k_{bg} = 4.75 \times 10^{-8}$ s^{-1} (pH = 7.4), see Ref. [84]. The pH value refers to the water that was previously buffered and then mixed with the cosolvent; [i] the background transesterification rate in this solvent mixture is given by the following expression: $k_{bg} = 10^{(pH-17.2)}$, see Ref. [53]; [j] the autoprotolysis constant in this mixture is $K_w = 10^{-18.4}$ and the neutrality is 9.2, see Ref. [51, 124]. [k] The acceleration reported by the authors is 3.0×10^3. [l] The acceleration reported by the authors is 3.2×10^4. [m] the background transesterification rate was calculated on the basis of literature data and the use of Eyring equation. [n] extrapolated at 1 mM concentration of dendron/dendrimer. [o] Extrapolated at 1.0 mM concentration of active unit (TACN). [p] This value was calculated through the following data: $k_2^{OMe} = 2.6 \times 10^{-3}$ and the autoprotolysis constant in MeOH, i.e. p[H+][-OMe] = 16.6. see Ref. [108]; [q] linear dependence on the catalyst concentration whithin the investigated concentration range. [r] calculated using the background reaction extrapolated with the Eyring equation. [s] The acceleration has been extrapolated at 1.0 mM active units, i.e. guanidine/ium, concentration. [t] $k_{bg} = 7.9 \times 10^{-8}$ s^{-1}. [u] $k_{bg} = 6.4 \times 10^{-7}$ s^{-1} extrapolated with Eyring equation. [v] $k_{bg} = 2.0 \times 10^{-7}$ as reported by the authors, see Ref. [135].

[S] the substrate concentration. The total catalyst concentration is given by $[C]_T = [C] + [CS]$. In the case $[C] >> [S]$ or $[C] >> [CS]$ the free catalyst concentration in Eq. (6) can be replaced by $[C]_T$.

$$k_{obs} = \frac{k_{cat}K_b[C] + k_{bg}}{K_b[C] + 1} \quad (6)$$

$$v = k_{obs}[S] \quad (7)$$

In a saturation kinetic experiment with a reaction mechanism as that in Eq. (3), either the catalyst or the substrate concentration can be varied. Unlike in a Michaelis-Menten kinetic analysis of natural enzymes, it is common for supramolecular catalytic systems to carry out the experiments with an excess of catalyst, even when the catalyst can operate with a good turnover, and to vary the catalyst concentration in saturation experiments. This practice is frequently employed in the literature in order to decrease the kinetic run times and avoid substrate/product inhibition.

Whenever the k_{bg} is neglected and the experiments are conducted under subsaturating concentrations, meaning that a small percentage of substrate is bound to the catalyst, i.e. $K_b [C]_T << 1$, the expression of the reaction rate is given by Eq. (8). In a number of literature reports, the catalyst concentration was not systematically varied and therefore it is not possible to evaluate the binding constant K_b and k_{cat} separately, but just their product k_2, defined in Eq. (9) as a second-order rate constant.

$$v = K_b k_{cat}[C]_T[S] \quad (8)$$

$$k_2 = K_b k_{cat} \quad (9)$$

In Tables 1 and 2 are reported the value of k_{obs} for all the discussed catalysts measured at the concentration used by the authors in the experiments. However, as k_{obs} value is strictly dependent on the catalyst concentration, see Eq. (6), it is not meaningful to use this parameter to compare the intrinsic efficiency of the catalysts. Since there is a linear dependence of k_{obs} on the catalyst concentration under subsaturating conditions, it is sound to compare the k_2 values to provide an idea of the absolute reactivity of the discussed systems. The values of k_2 reported in Tables 1 and 2 and discussed in the text, were calculated, in the cases in which the authors do not provide them directly, through Eq. (9), for

Table 2
Kinetic Data for the Cleavage of BNPP promoted by the listed catalyst [a].

Entry	Catalyst	k_{obs} (s^{-1}) [b]	$k_{rel} = k_{obs}/k_{bg}$ [c]	k_2 (s^{-1} M^{-1})[d]	K_b [e] (M^{-1})	k_{cat} [e]	Conditions	Refs. [f]
1	TACD-Zn^{II}	4.0×10^{-7}	180 [g]	8.5×10^{-5}	–	–	pH > 8 [h] $T = 35$ °C, $I = 0.2$ M	[37]
2	TACN-Cu^{II}	3.4×10^{-7}	870	2.6×10^{-4}	–	–	pH = 7.2, $T = 50$ °C	[172]
3	**51**-La^{III}	6.4×10^{-5}	18	6.4×10^{-3}	< 150	–	pH = 10.5 25 °C [cat] = 10 mM	[162]
4	cyclen-Co^{III}	4.6×10^{-3}	1.5×10^{6}	4.6×10^{-1}	–	–	pH = 7.0, 50 °C [cat] = 10.0 mM	[39]
5	**52**-$(Zn^{II})_2$	4.2×10^{-6}	12 [i]	4.2×10^{-3}	–	–	pH = 10.5, 25 °C	[163]
6	**53**-$(Zn^{II})_2$	1.9×10^{-6}	400 [j]	1.9×10^{-3}	–	–	pH > 9, $T = 35$ °C I = 0.2 M	[173]
7	**54**$_2$-$(Fe^{III})_2$	2.0×10^{-9}	180	2.1×10^{-5}	33	6.2×10^{-7}	pH = 8.0 25 °C	[174]
8	**32**-Zn^{II}	9.7×10^{-5}	6.0×10^{6} [k]	9.7×10^{-2}	–	–	pH = 7.0 T = 35 °C	[156,164]
9	**37**-Zn^{II}	2.2×10^{-5}	2.0×10^{5}	2.2×10^{-2}	–	–	pH = 8.0, $T = 25$ °C	[115]
10	**55**-$(Zn^{II})_2$	2.2×10^{-7}	720	2.2×10^{-3}	100	2.2×10^{-5}	pH = 8.8, 35 °C	[49]
11	β-CD + Eu^{III}	6.0×10^{-4}	2.7×10^{6} [n]	0.30	–	–	pH = 8.0, 25 °C	[87]
12	**41a**-Cu^{II}	1.0×10^{-5}	6400	5.0×10^{-3}	–	–	pH = 7.0, T = 50 °C	[125]
13	**41b**-Cu^{II}	7.0×10^{-6}	3200	3.5×10^{-3}	–	–	pH = 9.0 25 °C DMSO/H_2O 80 % [o]	[175]
14	**42b**-Cu^{II}	1.9×10^{-4}	2.2×10^{6}	0.38	–	–	pH = 8.9 25 °C DMSO/H_2O 80 % [o]	[126]
15	**56**	4.7×10^{-7}	1100	4.7×10^{-4}	–	–	pH = 9.3, 25 °C DMSO/H_2O 80 % [o]	[159]
16	**57**	4.4×10^{-5}	6.5×10^{4}	4.4×10^{-2}	–	–	pH = 9.5, 25 °C DMSO/H_2O 80 % [o]	[165]
17	**58a**-$(Zn^{II})_2$	1.3×10^{-6}	1.2×10^{4} [n]	1.3×10^{-3}	–	–	pH = 8.0, 25 °C	[168]
18	**58b**-$(Zn^{II})_2$	2.4×10^{-3}	3.3×10^{5} [p]	24	–	–	pH = 7.4, 25 °C	[167]
19	**59**-$(Zn^{II})_x$	1.0×10^{-5}	6.9×10^{5} [l]	1.5	4.7×10^{4}	3.2×10^{-5}	pH = 7.0 T = 35 °C [cat] = 1.0×10^{-5} M [m]	[169]
20	**43**	1.9×10^{-5}	2.4×10^{5}	0.57	2.0×10^{4}	2.9×10^{-5}	[cat] = 1.0×10^{-4} M	[127]
21	**61**- Cu^{II}	1.9×10^{-4}	–	1.9			pH = 7.5 T = 37 °C [cat] = 1.0×10^{-5} M, H_2O/EtOH 3:1	[171]

[a] solvent = water unless otherwise stated. [b] The k_{obs} values were typically measured with the initial rate method according to the following expression: $k_{obs} = v_o/[BNPP]$; experimental error for the rate constants ranges from 5 to 15 %. The k_{obs} values refer to the measurement at an actual catalyst concentration chosen by the authors in the experiments. If the experiments were conducted at different catalyst concentrations, the most representative concentration value was chosen. Whenever the catalyst concentration was not explicitly indicated by the authors, the k_{obs} value has been calculated from the k_2 or from Eq. (5) at 1.0 mM catalyst concentration. [c] Estimation of the BNPP hydrolysis rate in water at 50 °C is $k_{bg} = 3.0 \times 10^{-10}$ s^{-1}, see Ref. [39]) In the case the measurement was carried out at slightly different pH, *e.g* pH = 7.2 entry 2, the k_{bg} value was extrapolated assuming a linear dependence on $[OH^-]$. For entry 3: $k_{bg} = 3.5 \times 10^{-7}$ s^{-1}. For entry 5: $k_{bg} = 1.1 \times 10^{-10}$ s^{-1}, for entry 9: $k_{bg} = 1.1 \times 10^{-10}$ s^{-1} for entry 10: $k_{bg} = 2.8 \times 10^{-9}$ s^{-1}, entry 12: $k_{bg} = 7.8 \times 10^{-10}$ s^{-1}. The acceleration factor $k_{rel} = k_{obs}/k_{bg}$ has been linearly extrapolated to 1.0 mM catalyst concentration, also for those catalysts that were tested at slightly different concentration. The accelerations over the background reaction are reported with two significant figures; [d] for the catalysts that were not investigated in a *pesudo* Michaelis-Menten experiments, the k_2 values were approximately determined with the following equation: $k_{2=} k_{obs}/[C]_T$, where $[C]_T$ is the catalyst concentration. For the others k_2 values were determined as $k_{2=} k_{cat} K$. [e] These values were omitted in the case no saturation kinetic experiments has been carried out by the authors and consequently no catalyst-substrate binding constant can be determined. The error limit on the binding constant can be considered in the order of ±20%. [f] Reference to the article, see reference list at the bottom of the manuscript. [g] The background hydrolysis rate at 35 °C has been extrapolated on the basis of data measured at higher temperature, see Ref. [39]: $k_{bg} = 4.7 \times 10^{-10}$ s^{-1} at pH = 8.0; [h] the authors report only the second-order rate constant for the metal complex with the bound water molecule in its deprotonated form. [i] $k_{bg} = 3.5 \times 10^{-7}$ s^{-1}, extrapolated at pH = 10.5 from the data at pH = 7.0, Ref. [39]. [j] $k_{bg} = 4.7 \times 10^{-9}$ s^{-1} at pH = 9.0. [k] $k_{bg} = 1.6 \times 10^{-11}$ s^{-1} as reported by the authors [156]. [l] $k_{bg} = 4.5 \times 10^{-11}$ s^{-1}. [m] Concentration of the active units. [n] $k_{bg} = 1.1 \times 10^{-10}$ s^{-1} extrapolated at pH = 8. [o] The autoprotolysis constant in this mixture is $K_w = 10^{-18.4}$ see Refs. [51,124] for entry 13: $k_{bg} = 1.1 \times 10^{-9}$ s^{-1} extrapolated from pH 7.0, for entry 14: $k_{bg} = 1.7 \times 10^{-10}$ s^{-1} for entry 15: $k_{bg} = 4.3 \times 10^{-10}$ s^{-1} for entry 16: $k_{bg} = 6.8 \times 10^{-10}$ s^{-1}. [p] As reported by the authors.

those literature contributions that reports the values of k_{cat} and K_b. For those supramolecular systems for which the values of k_{cat} and K_b are not available, the corresponding k_2 value was estimated through the following equation: $k_2 = k_{obs}/[C]_T$, assuming a linear dependence of k_{obs} on the catalyst concentration. On this regard see also note *d* of Table 1.

In Tables 1 and 2, the accelerations k_{rel} are also reported, defined as the dimensionless ratio k_{obs}/k_{bg}. This is another important parameter to use in a comparison to evaluate the performance of an enzyme mimic. These values of k_{rel} were all calculated using k_{obs} at the typical catalyst concentration of 1.0 mM, see note *c* in Table 1.

3. Enzymes for phosphodiester bond cleavage and their mechanisms

Enzymes able to promote phosphoryl transfer reactions are an extremely heterogeneous class of proteins and can be classified according to different criteria [4,54–56]. A possible classification involves addressing the question of whether the reaction proceeds via an intermediate featuring a covalent bond between the phosphate and the enzyme or the phosphoryl unit is directly transferred to a substrate [57]. The side chains of several amino acid, provided with nucleophilic units, were proved to be involved in the formation of a phosphorylated enzyme intermediate. Among them, serine, threonine, cysteine and tyrosine can be mentioned [1,57]. Another criterion in the classification aims at determining whether the mechanism of cleavage follows a stepwise pathway or a concerted one. In the latter case the geometry features a pentacoordinated phosphorous atom as a transition state. This mechanism is often referred to as $S_N2(P)$ in the literature [58], for its strict analogy to aliphatic nucleophilic substitution. On the other hand, if the pentacoordinated intermediate is a minimum of energy, the mechanism is named A_N+D_N, whereas, in the case the departure of the leaving group precedes the nucleophilic attack, it is classified as D_N+A_N [54,59,60]. Other differences among this class of enzymes are the number and the nature of active units in the active site directly involved in the catalytic event. A selected examples of the best-known and representative enzymes in this category are the following:

i) *Eco*RI endonuclease [56] – a single ion directly involved in the catalysis, i.e. Mg^{II}; *ii*) alkaline phosphatases [61,62], containing two Zn^{II} ions in the active site; *iii*) IPpoI endonuclease with a single metal ion in the active site and a histidine acting as a general base [63]; *iv*) RNaseA presents a transition state stabilization where two histidines are involved, one acting as general base and the other as general acid facilitating the leaving group departure [64]. Additionally, a lysine unit stabilizes, with its charged side chain, the phosphate of the substrate.

In many metal-containing enzymes there are several residues such as aspartate or glutamate involved in the complexation of the metal cations. This experimental picture inspired many scientists to design a heterogeneous series of artificial phosphodiesterase models to mimic Nature. In the next sections we will organically and exhaustively comment on the strategies employed and on the kinetic data in HPNP and BNPP cleavage.

4. Artificial phosphodiesterases based on metal ions

Metal ions, complexed by proper ligands, are active units also in many man-made enzymes and in some cases they exhibit a meaningful activity even in the absence of complexing agents [65–68]. There are several plausible mechanisms to explain the activity of metal cations [24,69,70], e.g. Zn^{II} and Cu^{II} (see Fig. 1): *a*) the metal cation interacts with a water molecule, or a protic solvent molecule, significantly decreasing its p*K*a and consequently generating an active nucleophile even at relatively low pH value; *b*) the metal ion interacts trough an electrostatic/Lewis acid-base interaction with the oxygen atoms of the phosphate unit, reducing the amount of negative charge onto the phosphorous atom and, as a consequence, facilitating a nucleophilic attack onto this center; *c*) in a bifunctional mechanism both the operating modes described in points *a* and *b* are active and the transition state consists in a four-membered cyclic species; *d*) the deprotonated solvent molecule acts as general base toward the hydroxy unit in 2' position enabling an intramolecular nucleophilic attack of this unit on the phosphorous atom (for HPNP and RNA); *e*) in another possible operating mode, the metal cation interacts with an oxygen atom of the leaving group facilitating its departure. The latter mechanism can be simultaneously operating with mechanisms *a*-*d*, especially in the case of di- and multimetallic catalysts, and it is more likely to be operative in the presence of poor leaving group on the substrate (DNA or RNA) [59,60] and not in the case of BNPP and BNPP, that feature the *p*-nitrophenol as leaving group. Furthermore, another possibility is that a water/solvent molecule can act as mediator in mechanisms *a* and *e* as illustrated in Fig. 1 (*f* and *g*).

These mechanism of cleavage of HPNP and BNPP were also investigated in silico promoted both by metal cations and by other

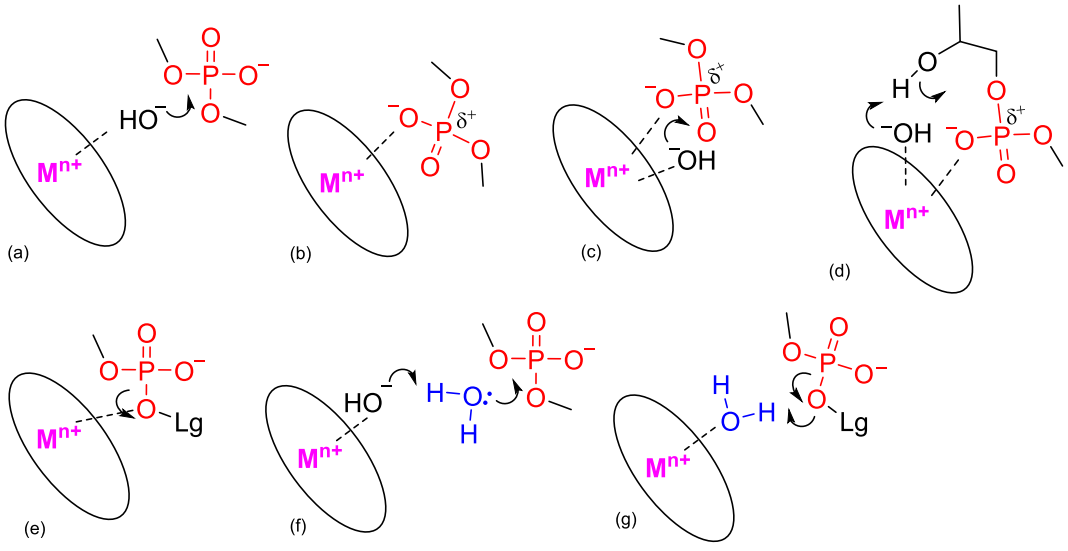

Fig. 1. Postulated metal cation operating mechanisms in the cleavage of phosphodiesters: *a*) nucleophile carrier; *b*) Lewis acid/base electrophilic activation; *c*) nucleophile carrier and simultaneous electrophilic activation; *d*) general base and electrophilic activation in a substrate with an intramolecular nucleophilic unit; *e*) leaving group departure assistance; water molecule intermediation in *f*) nucleophile generation and *g*) leaving group departure.

functionalities [70–76].

In Chart 1 are reported the structures of a few of the simplest metal-based phosphodiesterases based on a single metal center. Catalyst **1** and **2** [77], based on a pyridine units, exhibit a moderate activity toward HPNP (entries 1 and 2, Table 1). A higher activity is observed in the case of **3** and **4** [77,78], featuring two benzimidazole units involved in the complexation of the metal cation.

E. Kimura and J. Chin et al. were among the first who established the use of macrocyclic polyamines as active units in the cleavage of phosphoric diesters [37,39]. These ligands show the ability to complex a wide variety of metal cations with high binding constant [16,79,80] and to follow the activation modes illustrated in Fig. 1. The nucleophilicity of the nitrogen atom of the macrocycle allows a straightforward functionalization with side arms and therefore the possibility to realize multifunctional enzyme mimics featuring two or more metal centers, other active units or recognition sites. The most representative aza-macrocyclic structures are the triazacyclododecane (TACD, **5a**), triazacyclononane (TACN, **5b**) and the cyclen (**5c**). They show a significant catalytic activity both as Zn^{II} and Cu^{II} complexes [81–83], as highlighted in entries 5–8 of Table 1, while in the case of the Ni^{II} the phosphodiesterase activity is hardly detectable [82] (entry 9).

An alternative to these macrocycles is the 2,6-bis(*N*,*N*-dimethylamino)pyridine (BAMP), **5d**, that has been successfully used in polymetallic catalysts, *vide infra*. Although its activity is fairly good, its binding constant with Zn^{II} and Cu^{II} is around 10^4 [84,85], and therefore it does not guarantee a quantitative complexation at submillimolar catalyst concentration. Monometallic Ce^{III} and La^{III} complexes of cyclen derivatives, show in a few cases a noteworthy activity toward HPNP, with accelerations over the spontaneous reaction at the same pH exceeding four orders of magnitude [86] (entries 11 and 12, Table 1). The activity of these systems is attributable, in large part, to an intrinsic reactivity of the lanthanum itself in this reaction [65,87].

The Cu^{II} complex of **8** is still active in the transesterification reaction [88] while the more structured **9**, tested at more basic pH, does not show a relevant activity [89]. A different approach in the design of nitrogen-based ligands is illustrated by the triaminocyclohexane **10a** and its conformationally more rigid derivative **10b** [90]. The latter ones accelerates the HPNP cleavage of 170-fold with Cu^{II} and in a very similar way with Zn^{II}.

An important step forward in the design of artificial phosphodiesterases, and supramolecular catalysts in general, is the development of di- and multifunctional systems. For this reason, several research groups have oriented their efforts at the synthesis of ligands able to bind more than a metal cation (Chart 2).

An attempt to realize a bimetallic artificial phosphodiesterase has been reported by Mancin et al. However, the *meta* and *para* phenylene derivatives **11a** and **11b** [91] do not overcome the reactivity of their monofunctional counterpart (Table 1, entries 16–20). On the other hand, the bimetallic Cu^{II} complex of **12** [92], consisting of two triazamacrocyclic units conformationally constrained by an aromatic ring, exhibits an important catalytic activity in HPNP transesterification at pH 7, with a rate acceleration of 3600-fold. The tritopic ligand **13** [93], provided with three *N*,*N*-bis(2-pyridylmethyl)ethylenediamine pendants, as Zn^{II} complex is able to catalyze the HPNP transesterification. Its lower performance is probably attributable to an higher mobility and, as a result of that, a lower preorganization. Similar considerations also apply to ditopic compound **14** [94,95]. In the case of bimetallic catalysts, on the basis of the kinetic data and cooperativity obtained from the comparison with the activity of the monofunctional models, essentially two metal cations are involved in the HPNP transesterification [40,81,84], one of them acting as general base through a deprotonated solvent molecule, and the other one acting as Lewis acid activator, according to the mechanism depicted in Scheme 2. Interestingly, the cooperativity between metal centers can be reached also through metal clusters as proved in the case of the polyoxomolybdate $[Mo_7O_{24}]^{6-}$ (**15**, Table 1, entry 24) [34], zirconium [33] and lanthanum [65,87,96].

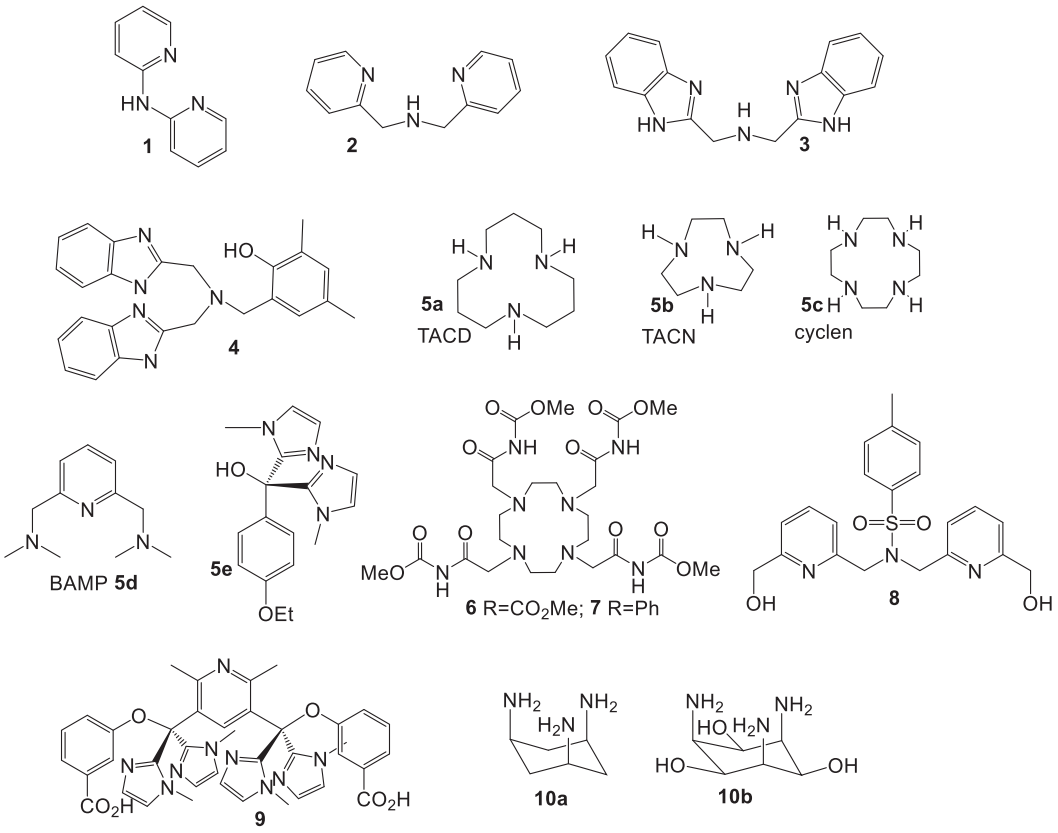

Chart 1. Examples of ligands and macrocycles able to complex a single metal ion.

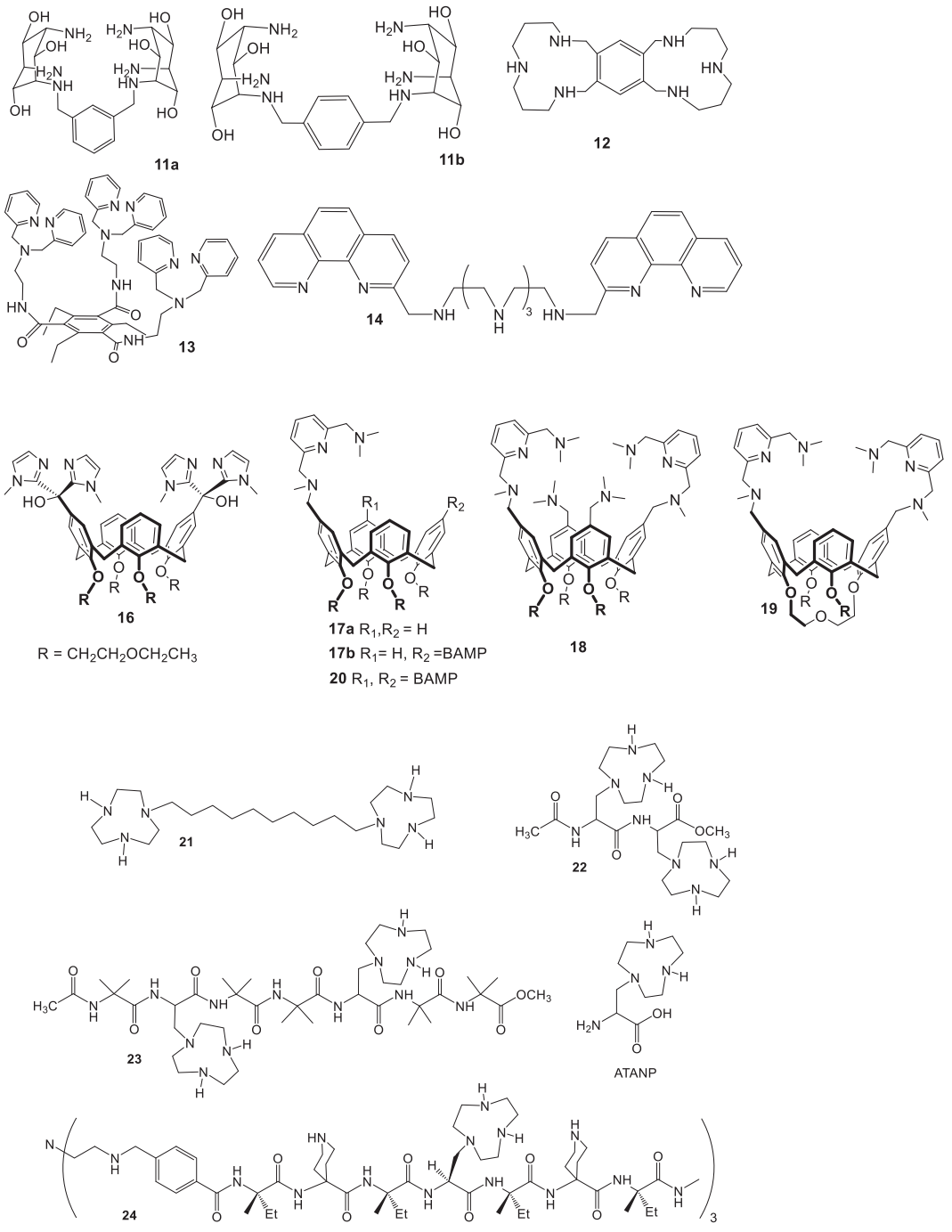

Chart 2. Bi- and polymetallic precatalysts.

A significant step forward was introduced by Reinhoudt and coll. with the use of calix[4]arenes [97]. This macrocycle does not present a sufficient binding space in the cavity, however its usefulness lies in its partially inhibited conformational mobility. Indeed it is a good compromise between preorganization and flexibility [76,98]. The metal complexes of calixarenes **16** and **17b**, based on bis-imidazoyl and BAMP ligands respectively [97], turned out to be extremely efficient in the HPNP transesterification with acceleration ratios exceeding four orders of magnitude. In addition, they exhibit remarkable cooperativity whenever their cleavage rate is compared with those of their mono-metallic models **5e** and **17a**.

The addition of two tertiary amine functionalities in **18** does not provide an increase of the reactivity [99] as well as the functionalization at the upper rim with an additional ligand as illustrated by compound **20** (Table 1, entry 32) [84,100]. In the latter case, the absolute reactivity is slightly higher than that observed for the corresponding bimetallic catalyst. This modest superiority, likely attributable to a statistical advantage, does not indicate the simultaneous cooperation of three metal centers. The alkylation at the lower rim in calixarene **19** [100], with a consequent reduction of the mobility, results in a lower catalytic activity compared to **17b**. This evidence strongly points to the existence of a crucial conformational mobility in calix[4]arenes that has a strong impact on the catalytic activity. Another noteworthy example that illustrates the primary role of preorganization is provided by Scrimin,

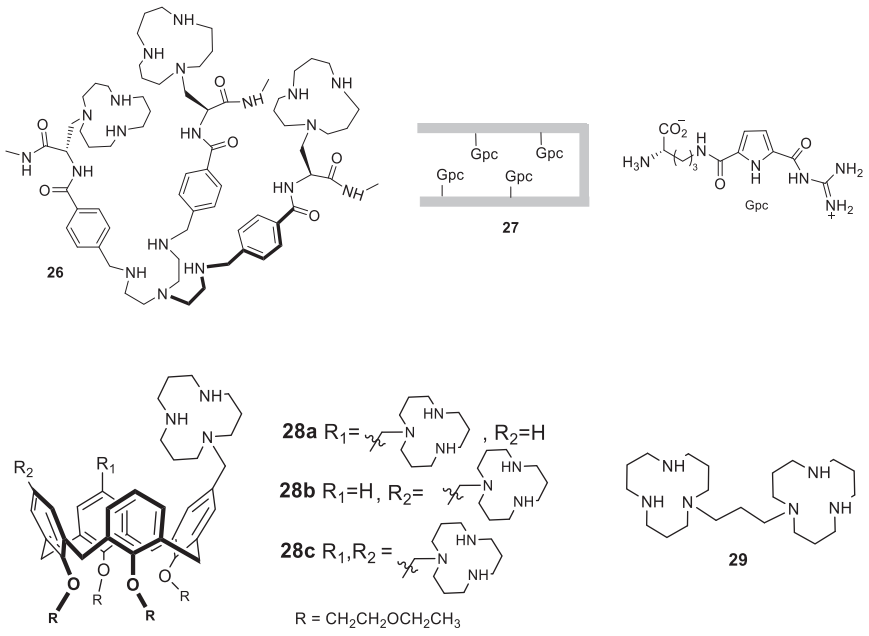

Chart 2. (*continued*).

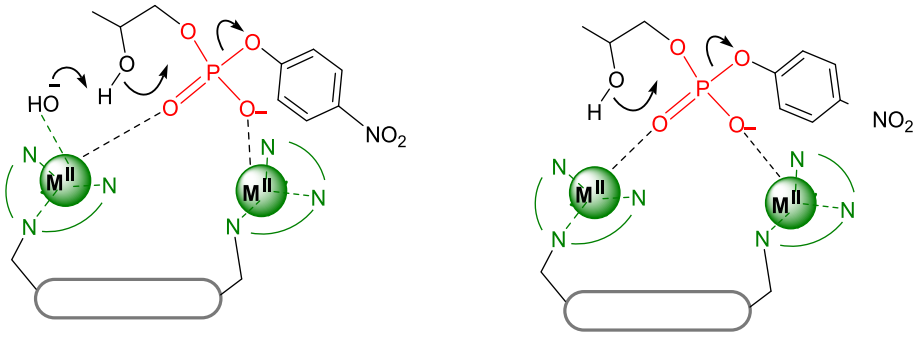

Scheme 2. Possible operating modes for the bimetallic catalysis in HPNP: Lewis acid activation and a complexed hydroxide ion acting as a general base according to mechanism *d* in Fig. 1 (left). Alternatively, double Lewis acid activation (right).

Mancin and their coworkers [101]. The floppy C_{10} alkyl chain in ditopic ligand **21**, based on the triazacyclononane unit, does not allow an appropriate cooperation of the two active units. The second order rate constant for the cleavage in the presence of this bimetallic complex, i.e. 0.15 s^{-1} M^{-1} (Table 1, entry 33), is only 3-fold that of TACN-Zn^{II} in the same conditions [102]. Taking into account that **21**-$(Zn^{II})_2$ bears two TACN-Zn^{II} units, this evidence indicates that the two metal centers act in a quasi-independent way. On the other hand, the addition of *β*-cyclodextrin at 5 mM concentration results in an increase of reactivity by a factor of 30 comparing the second order rate constants (Table 1, entry 34). The formation of a more preorganized complex between **21**-$(Zn^{II})_2$ and the cyclodextrin involving its cavity was confirmed with experiments carried out at increasing concentration of *β*-CD, indicating an evident host-guest allosteric control in this system.

A different approach in the design of bimetallic supramolecular catalyst was attempted through the use of peptides and peptidomimetics [82,83,103–105]. Complexes of different metal cations with the ditopic peptidomimetic ligand **22** do not exhibit a relevant catalytic activity likely ascribable to a short distance of the two TACN units that does not allow an optimal orientation of the two catalytic groups [82]. A slightly higher activity is experienced in the presence of metal complexes of ditopic ligands **23** [82] and **24** [103]. The same group reported about the unnatural peptides **25a–c** [83]. Their chains are known to fold into a hairpin helix-loop-helix motif. In their sequences are present four residues of the artificial amino acid ATANP for **25a** and two for **25b** and **25c**. Their tetrametallic and bimetallic Zn^{II} complexes reach two orders of magnitude of acceleration (entries 42–44). A further development has been achieved with the tripodal ligand **26** [105]. This compound is able to complex three Zn^{II} cations with the TACN units, and a forth Zn^{II} though interactions with the secondary and tertiary amines at the center of the structure. In this case the acceleration ratio overcome three order of magnitude (Table 1, entry 45) and, in addition, kinetic data strongly points to the existence of an allosteric effect [105]. Among this kind of catalysts, compound **27** is noteworthy [104]. This peptide mimic the arginine-based enzymes with four guanidinocarbonyl pyrrole units. The peptide chain is able to form two distinct α-helix domains that result in a U-shaped conformation with the active units pointing toward the inner space. The catalytic measurements carried out in the presence of this species highlight a fair catalytic activity in the cleavage of HPNP. Further comments about the role of guanidinium units in these catalysts are discussed in the next Section.

Another indication of the convenience and versatility of the calixarene scaffold is provided by catalyst **28a–c**, featuring two or three TACD units at the upper rim of the scaffold [81]. The Zn^{II} and Cu^{II} complexes of these ligands turned out to be effective in the cleavage of the RNA model. In the case of the Cu^{II} complexes there is a notable difference, in terms of efficiency between the 1,2- and 1,3- functionalization at the upper rim of the calixarene, namely nearly 27-fold (Table 1,

entries 50–51). This evidence highlights the extreme sensitivity of the catalytic efficiency to the ligand geometry and functional groups orientation. Interestingly, in the comparison of the accelerations k_{rel} and second order rate constants k_2, the trimetallic catalyst **28c**-$(Zn^{II})_3$ overcomes the corresponding bimetallic **28**-$(Zn^{II})_2$ by an extent that exceeds the statistical factor and the experimental error. This observation is in agreement with the existence of a trimetallic mechanism consisting in a synergistic cooperation of three metal cations in the reactive event [81].

The simple ligand **29**, consisting of two TACD units linked by a propylene chain, was studied as phosphodiesterase in methanol by Stan Brown and his coworkers [71,106,107]. This compound exhibits the most astonishing catalytic effect both in terms of absolute reactivity and acceleration. The k_{rel} value in this solvent mixture at pH 9.8 is close to 10^{12} (see entry 53 and note *p* to Table 1 and Ref. [106–108]). This surprising catalytic effect is attributed to an excellent synergism between the metal centers, an optimal affinity for the transition state of the reaction and a medium effect generating a reduced polarity/dielectric constant. According to the X-ray structure of the complex, it is possible to postulate the presence of a bridging methoxide ion between the two Zn^{II} centers that probably plays a crucial role in the catalysis. To the best of our knowledge, this is the most effective artificial phosphodiesterases ever reported for this substrate and, with an enzyme-like acceleration, definitely among the most effective catalytic supramolecular systems in general [12]. The activating effect of methanol as solvent has also been observed for other metal complexes [109], even for catalysts with a lower level of preorganization [110].

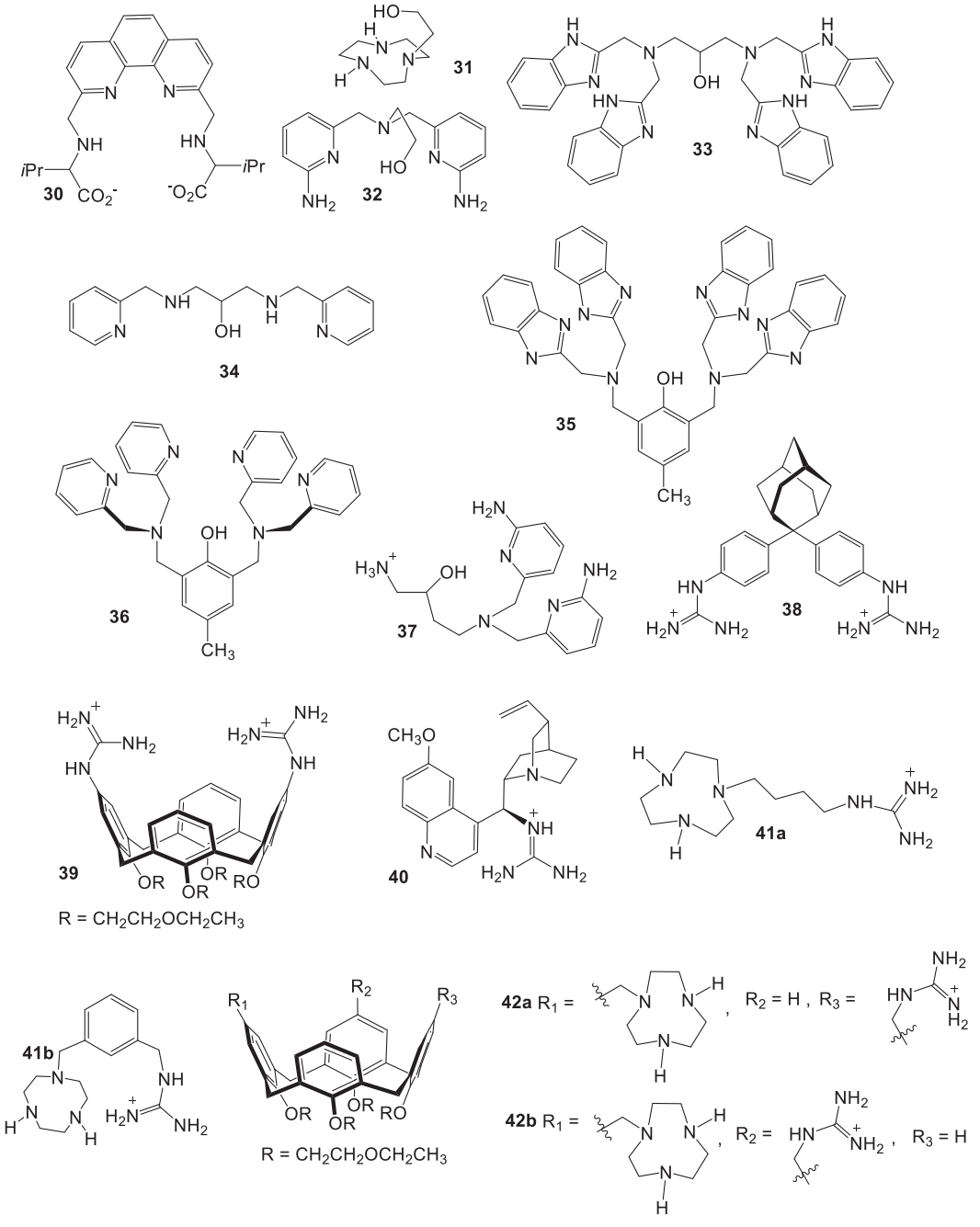

Chart 3. Heterofunctional precatalysts.

5. Heterofunctional artificial phosphodiesterases

This section covers the use of other chemical functions, either acting independently or in conjunction with metal ions, in the design of this kind of catalysts. Examples are given in Chart 3. In Table 1, in entries 54 and following, are reported a few examples of phosphodiesterases provided with other active functions, in addition to metal ions. The phenanthroline derivative **30** features two ammonium units in close proximity to the metal center [111]. However, their presence does not affect in an important way the catalytic performance. Also in the complex **31**-Zn^{II}, the presence of a hydroxy unit close to the cation and potentially able to directly interact with it, does not increase too much significantly the activity of the TACN unit (Table 1, entry 55) [14,112,113]. On the other hand, the proximity of hydroxy groups in complexes of ligands **32**–**36** results in a significant increase in the observed reaction rate and catalytic acceleration k_{rel}. In the case of **35**-$(Cu^{II})_2$ the k_{rel} value is as high as 76,000 [78], with an impressive advantage over its corresponding monometallic analog **4**-Cu^{II} (entry 4, Table 1) and therefore exhibiting an extremely high cooperativity between the two metal centers. Although the phenolic group can potentially act as a nucleophile, a hydrogen-bond donor and a general base, in the case of HPNP it is likely that only the latter mechanism is operating since the substrate itself, already features the presence of a nucleophile in its structure. A surprisingly high catalytic effect is reached by bimetallic Zn^{II} complex **36**-$(Zn^{II})_2$ reported by Stan Brown and coworkers [114]. This catalyst exhibits an extremely high observed rate constant as well as an enormous acceleration ratio of 10^{10} [114]. The authors argue that the deprotonated phenolic O atom bridges the two metal ions (oxy bridge) and this might have a role in reducing the Zn^{II} – Zn^{II} repulsion and therefore in increasing the cooperativity of the two metal centers even at short distance. This effect, beneficial for the catalytic activity in water, was proved to impair the efficiency of the catalyst in methanol by comparison with analogs lacking the bridging oxyanion in their structural motif [114].

Mancin et al. reported about the reactivity of **37**-Zn^{II} toward the same substrate. This catalyst is provided with an ammonium unit that has turned out to be beneficial for the catalysis. This is demonstrated by the comparison with its analog (**32**-Zn^{II}) lacking the ammonium group (entry 56, Table 1) [115]. This beneficial effect can be ascribable to an electrostatic stabilization of the transition state through ammonium-phosphate interation, in addition to that exerted by the Zn^{II} unit.

In this context, a special focus should be dedicated to phosphodiesterases based on guanidinium. This cation is widespread in nature as it has the ability to interact to several oxoanions such as carboxylates and phosphates, due to geometric and electronic complementarity [74,116]. This group is definitely the most effective non-metal active unit, since other alternatives such as amine/onium [99] and imidazole [117,118] do not exhibit the same efficiency.

The binding constant between guanidinium and phosphate is not very high in water, $K_b < 10\ M^{-1}$ [119,120]. The reason is probably the high energy involved in the solvation of these ions. This interaction, in natural systems, typically occurs in hydrophobic pockets of enzyme where it is definitely stronger [116]. In supramolecular systems the drawback of a weak interaction can be overcome increasing the number of guanidinium units [51,121,122]. However, in the design of a supramolecular catalyst, a high binding constant with the substrate is not always essential, as the most important acceleration arises from a selective stabilization of the transition state.

Examples of systems exclusively based on guanidinium and lacking other active units are the adamantane derivative **38** [53] and the guanidinocalixarene **39** [51,123]. Both of them show a fair activity in the HPNP cleavage in DMSO/H_2O 80 %, even though lower in comparison with other efficient bimetallic phosphodiesterases. According to the data reported in the literature the guanidinium itself appears to be intrinsically less efficient than metal ions. The abovementioned DMSO/H_2O solvent mixture is convenient to study the reactivity of guanidinium-based system because it slightly increases the strength of phosphate-guanidinium association and inhibits the background reaction. It is also suitable to carry out potentiometric titrations to determine the distribution of the species at different pH values [51,123,124]. Kinetic experiments, carried out at different pH values, show a bell-shaped profile, with a maximum of activity at pH at which the prevalent species is that featuring a guanidinium ion and a guanidine unit. This experimental outcome suggests a mechanism in which the guanidinium is acting as electrophilic activator, and the guanidine as general base (see Scheme 3a).

An unconventional example of phosphodiesterase is compound **40** [52], whose catalytic mechanism is based on the synergistic action of a tertiary amine and a guanidinium. In this example the peculiarity is the use of the quinine scaffold. The catalyst is fairly efficient (entry 65, Table 1) and furthermore, because of its enantiomeric purity, is also active in the kinetic resolution of the two enantiomers of HPNP [52].

In the literature there are also examples of catalysts able to perform their catalytic activity with the combined action of a metal cation and a guanidinium unit, with the postulated mechanism illustrated in Scheme 3b. The simplest systems are based on a short alkyl chain, **41a** [125], and a *meta*-xylylene scaffold, **41b** [43,117]. The latter, despite its structural simplicity, shows remarkable k_{rel} values both as Cu^{II} and Zn^{II} complex. Another relevant step forward, also in this case, has been introduced by the calix[4]arene scaffold. Heterofunctional ligands **42a** and **42b** [41,126], featuring a TACN unit and a guanidinium at the upper rim in 1,3- and 1,2- positions respectively, turned out very active in the HPNP transesterification. In the case of the Cu^{II} complexes, the catalysts nearly reach an acceleration ratio of 6 orders of magnitude (entries 70 and 71, Table 1). These values are, as the best of our knowledge, the highest acceleration ever reported of a single-metal artificial phosphodiesterases. It is also relevant to note the significant difference of the performances of the 1,2- and 1,3- isomers both for Zn^{II} and Cu^{II} complexes. This represents another indication of the sensitivity of the transition state stabilization efficiency to small variations of the geometry and functional group orientations [41,126].

Interestingly, in a recent research article, Das group reported about short peptides able to assume cross-β amyloid stacks simulating the binding pocket of enzymes [127]. The dimer of peptide **43**, provided with a guanidinium and an imidazole function, shows a good activity in the cleavage of HPNP (entry 72, Table 1).

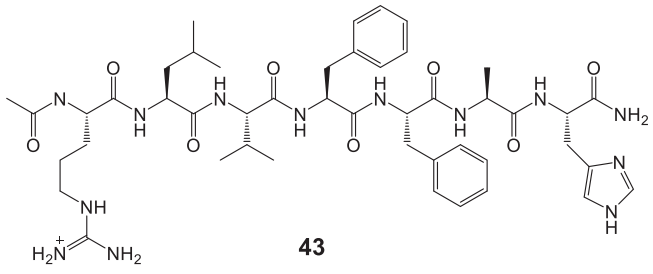

43

6. Artificial phosphodiesterases based on nanostructured materials

The primary issue with bi- and multifunctional catalytic systems is the necessity of time-consuming multistep synthesis. This inconvenience can be addressed using multivalent nanostructures and polymer-based supports (See Chart 4).

Scrimin, Prins et al. reported about the use of peptide dendrons and dendrimers functionalized at the periphery with TACN [128,129]. The cleavage of the RNA model compound in the presence of dendrimer **45** and dendron **44**, exhaustively complexing Zn^{II} ions, exhibits orders of magnitude acceleration ratio. These systems are able to perform a relevant catalytic activity at high dendrimer dilution, i.e. 600 nM. In

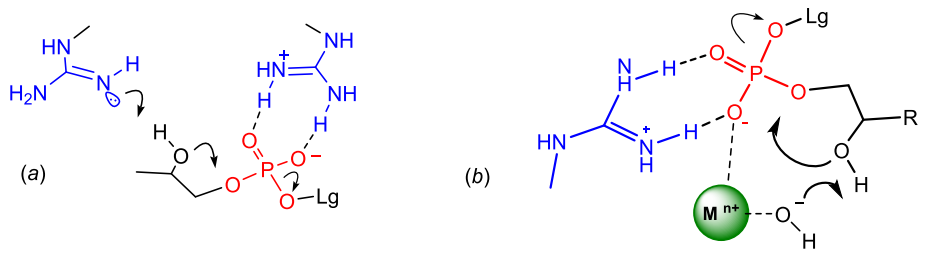

Scheme 3. Postulated mechanisms for the HPNP transesterification in the presence of two guanidine/ium units (*a*) and a guanidinium and a metal cation (*b*).

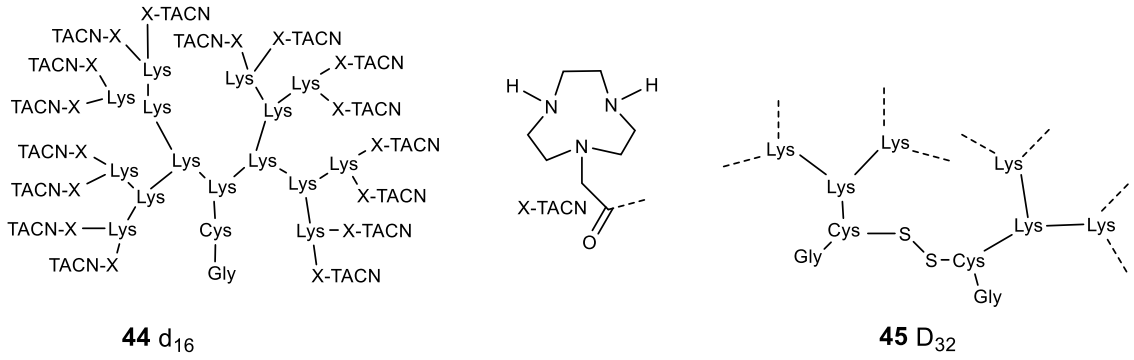

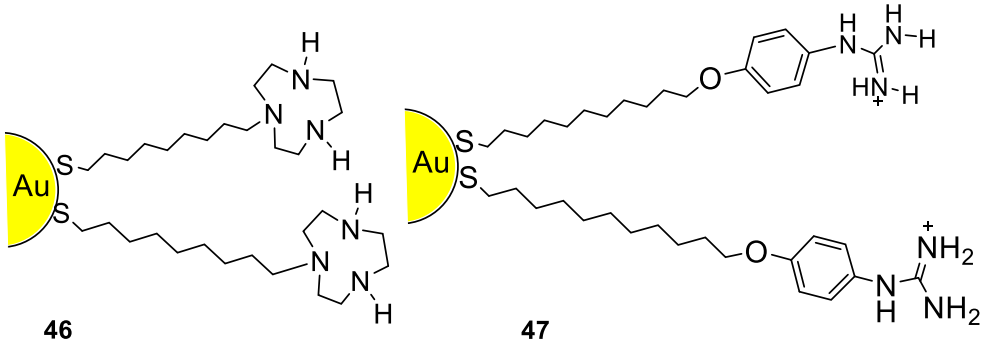

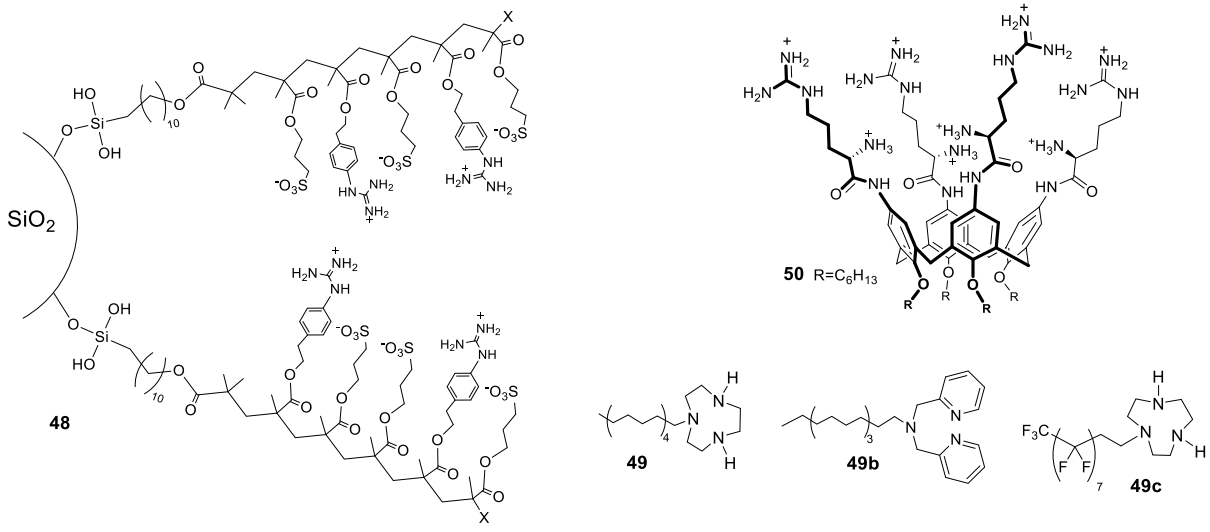

Chart 4. Precatalysts based on nanostructured supports or hydrophobic aggregates.

Table 1, entries 73 and 74, are reported the accelerations extrapolated both to 1 mM dendrimer concentration and to 1 mM TACN concentration. Based on the analysis of the pseudo-Michaelis-Menten profile and the K_b and k_{cat} values, the authors suggest that the observed positive dendritic effect does not need to be attributed to an enhanced association constant in the multivalent system or alterations in the local microenvironment at the interphases. Instead, the authors propose that the effective catalytic performance of these dendrimer-based catalysts is primarily driven by the system ability to create catalytic sites where multiple active units can work together, in a cooperative fashion, on the substrate to facilitate the catalytic process [128].

A similar synergistic effect of the catalytic units can be achieved via self-assembly of properly functionalized thiols on the surface of gold nanoparticles (Au NPs) [130–136]. Also this approach allows a very high level of cooperativity, whenever comparing the multivalent system with the activity of the same molecules in solution. An example is given by AuNPs **46** (entry 75, Table 1), passivated with a C_9 thiol functionalized with a TACN via *N*-alkylation. It was proved also that AuNP can be effectively employed to self-assemble thiols provided solely with guanidinium as in AuNPs **47** [133]. Also in this case, the system provides a relevant level of cooperativity even though the acceleration is lower than the metal complexes of TACN-based nanocatalysts, due to the lower intrinsic reactivity of this unit, as observed in the catalysts based on the conventional molecular scaffolds illustrated above.

Another possible approach for the fabrication of nanostructured catalysts is to exploit the versatility of polymer brushes [137,138]. These polymeric materials can be prepared via surface-initiated atom-transfer radical polymerization onto the surface of silica nanoparticles. With this strategy it is possible to fabricate hybrid materials like **48** [139]. It basically consists in silica nanoparticles provided with polymer chains decorated with guanidinium units. A suspension of these NPs exhibits a remarkable activity (entry 77, Table 1), with a relevant advantage, also in terms of effective molarity, over alternative systems based on guanidine/ium on AuNPs [133] and conventional molecular scaffolds [51,53,119] listed in Table 1.

In the absence of a nanostructured support there is the possibility to realize a multivalent artificial nanoenzyme thanks to the operation of hydrophobic effects that originate micelles and other aggregates [140–146]. A representative example is given by **49** in its aggregate form, showing a catalytic efficiency (entry 78, Table 1) that clearly benefits from the multivalent effect [143]. Compound **49b** also shows a remarkable cooperative effect as aggregate. In this case, the authors have proven that the addition of purine and pyrimidine nucleosides finely tune the catalytic activity altering the micellar structure [146]. Alternative to a conventional hydrocarbon chain, it is possible to use a polyfluoroalkyl chain to induce aggregation of TACN-Zn^{II} units such as in **49c** [147].

As a last example of nanostructured material useful in the design of phosphodiesterase mimics are nanodiamonds (NDs). They consist in a core of nanocrystalline diamond surrounded by oxidized carbon atoms on the surface, i.e. hydroxy and carboxylate groups [148,149]. The interest toward NDs is motivated by their versatility in a wide range of applications [148,150] and by their limited cytotoxicity unlike other carbon-based materials [150,151]. They feature also graphite-like domains, consisting of conjugated sp^2 carbon atoms [152]. The presence of all these functionalities grants them the ability to adsorb a wide range of chemicals through weak interactions [148,153]. A recent article proved that it was possible to immobilize onto NDs compound **50**, a calix[4]arene decorated with four arginine pendants [154]. Their catalytic properties in the cleavage of HPNP were investigated with an in-depth kinetic analysis and its performance compared with that of **50** free in solution and forming aggregates [142]. The experimental data demonstrate that this compound is firmly adsorbed onto the nanodiamond surface, through noncovalent interactions, and exhibits activity in the transesterification of the RNA model compound in water (entry 81). Interestingly, its performance when on nanodiamonds reveals a significant advantage over its catalytic activity at the same concentration in solution [154] The most promising features of the enzyme mimics based on this approach are their versatility and ease of preparation, avoiding more elaborated procedures required in the case of gold nanoparticles, polymers and dendrimers.

7. Hydrolysis of the DNA model compound

In this section a few relevant examples of phosphodiesterases able to cleave the bis(*p*-nitrophenyl) phosphate are presented, see Chart 5. *T*he corresponding kinetic data reported in Table *2*. Since there is no hydroxyl unit on the BNPP, the mechanism must necessarily include a hydroxide ion or a water molecule acting as external nucleophile (Scheme 4). The lack of the intramolecular nucleophilic group results in a spontaneous reactivity lower by two-three orders of magnitude, compared to its analog HPNP [126,159], similarly to the difference in reactivity between DNA and RNA [8,9,13]. This higher reluctance to hydrolysis entails longer reaction time and for this reason, in some cases, the kinetic experiments are carried out at higher temperatures, *i.e.* 35 and 50 °C. On the other hand, for the reason illustrated in the introduction, the substrate tends to be more sensitive to the presence of the catalyst exhibiting higher acceleration k_{rel}, as highlighted in Table *2*.

The hydrolysis of BNPP, similarly to HPNP, can be slightly accelerated by metal ions and clusters of them [33,34,160,161]. The addition to a BNPP solution at pH 7 of the Zn^{II} complex of triazacyclododecane (TACD, **5a**) and other cyclic polyamines does not improve the hydrolysis rate in an important manner (entry 1, Table 2) [37]. The absolute hydrolysis rate does not improve in the case of TACN-Cu^{II}. The La^{III} complex of the chelating agent **51** is also poorly effective, with an acceleration over the spontaneous reaction as high as 18 (entry 2, Table 2) [162]. Conversely, Chin et al. reported that the cobalt(III) complex of cyclen (**5c**) effectively catalyze the reaction with a k_{rel} of 10^6 [39].

The attempt to design a bimetallic catalyst with two TACN units in ligand **52** resulted in a poor catalytic factor [163]. A slight improvement was obtained with the Zn^{II} and Fe^{III} dinuclear complexes of ligands **53** and **54** that exhibit accelerations of two orders of magnitude (entries 6 and 7, Table 2). On the other hand, an important effect is observed for the heterofunctional ligand **32** previously discussed for its activity toward HPNP. In the presence of its Zn^{II} complex, the BNPP hydrolysis is enormously accelerated, both in terms of absolute reactivity and acceleration over the uncatalyzed cleavage (entry 8, Table 2) [156,164]. Notably, the analogous complex **37**-Zn^{II}, provided with an ammonium unit, is 30-fold less effective [115]. The reason is likely ascribable to the electron withdrawing properties of -NH_3^+ group that decreases the nucleophilicity and the coordinating ability of the hydroxyl group. The dinuclear Zn^{II} complex of **55**, provided with two β-cyclodextrin (CD) units, is more efficient in the cleavage of BNPP than HPNP [49]. This unusual behavior is attributed by the authors to a selective binding ability of the catalyst for the DNA model due to simultaneous complexation of each of the aromatic units of BNPP by the two CD cavities. This hypothesis is confirmed by the inhibition on the BNPP cleavage observed in the presence of increasing amount of di(*p*-tert-butylbenzyl) amine (DBBA), that, on the other size, does not affect at all the HPNP transesterification rate. Indeed, DBBA perfectly fits in the β-CD cavities, thus preventing the two *p*-nitrophenyl units of the substrate from being complexed [49].

Interestingly, the bare addition of Eu^{III}, and other trivalent lanthanides, to a β-CD solution resulted in the highest acceleration observed for BNPP cleavage among the systems considered in the present review (entry 11 of Table 2) [87]. The authors argue that the active species is a dinuclear polyhydroxocomplex of general formula $[Me_2(\beta\text{-CD})(OH)_n]_{6-n}$ with $n = 3$–5 [87].

The Cu^{II} complexes of heterobifunctional ligands **41a** [125] and **41b** [43], based on the simple butylene and *meta*-xylylene scaffolds respectively, demonstrate the efficacy of the combined dyad metal center/

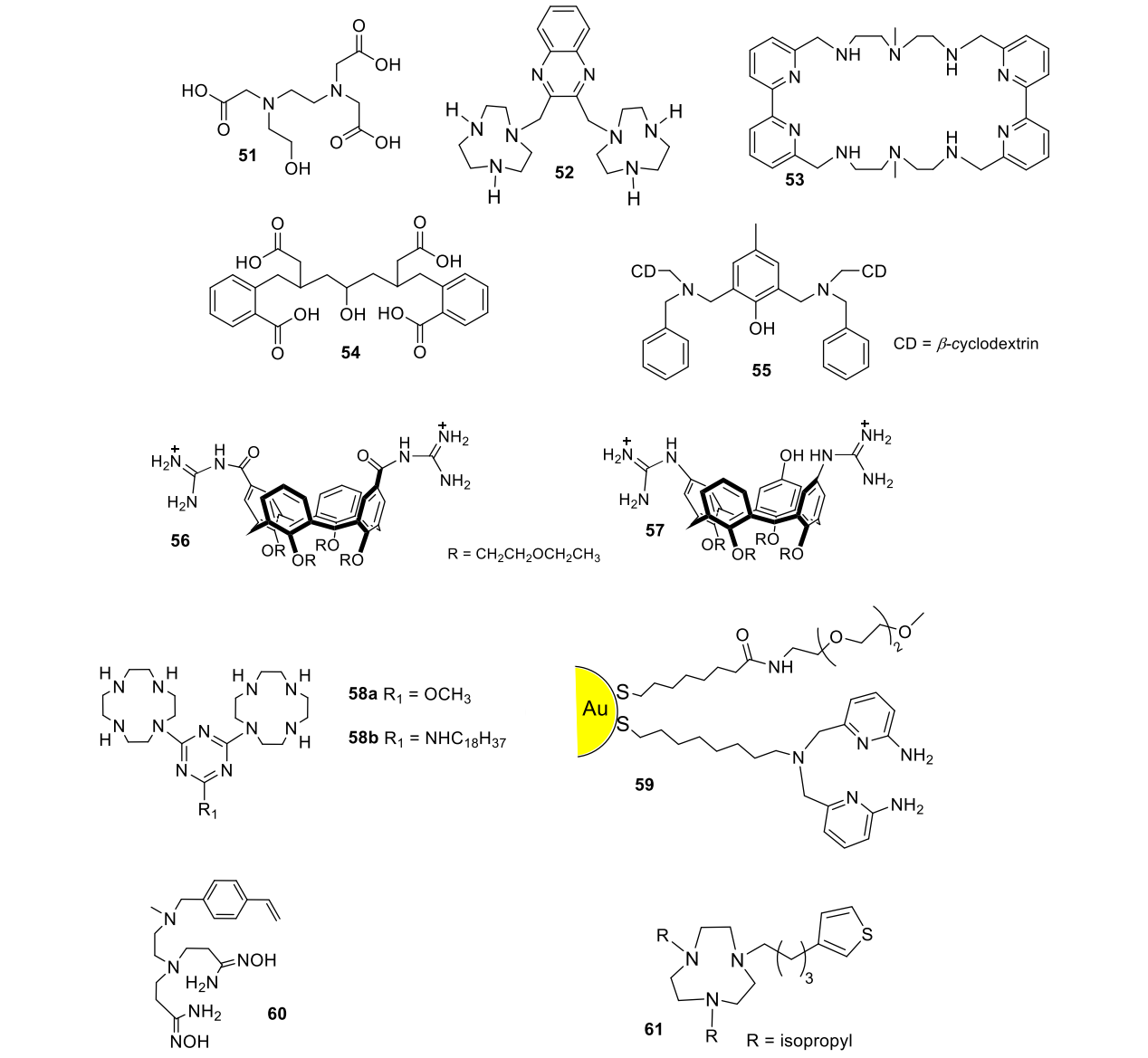

Chart 5. Precatalysts active in the cleavage of the DNA model.

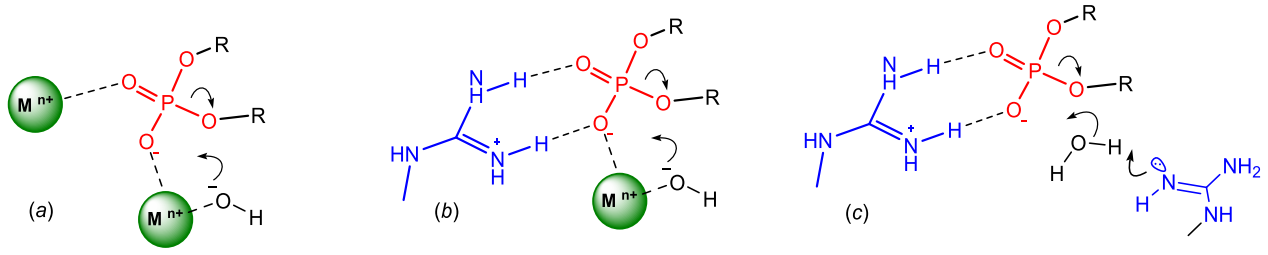

Scheme 4. Postulated bifunctional mechanisms for the BNPP cleavage promoted by metal ions and/or guanidiniums (R = *p*-nitrophenyl).

guanidinium in the hydrolysis of the DNA model, with accelerations around three orders of magnitude (entries 12 and 13, Table 2). The same active units, i.e. TACN-Cu and guanidinium, were employed in the calix[4]arene derivative **42b**-Cu^{II} (Table 2, entry 14) [126] where the BPPP cleavage rate was surprisingly enhanced to a k_{rel} value of 2.2×10^6. This system, together with the dimetallic europium/β-CD complex mentioned above are, to the best of our knowledge, among the most effective supramolecular catalysts for the cleavage of this substrate reported in the literature. The catalytic system solely based on guanidinium units, even though active, are not able to reach the acceleration mentioned above, as exemplified by the 1,3-diacylguanidinocalix[4]arene **56** [159]. However, the calixarene **57**, additionally provided with a phenol hydroxy group is 60-fold more effective than **56** [165]. The trifunctional catalyst **57** mimics the DNA Topoisomerase I, featuring

a tyrosine and two arginine residues in its active site [166]. Kinetic experiments unambiguously suggest an effective cooperation of the three active units and the involvement of the phenolate moiety as a nucleophile in a phosphoryl transfer step [165] with a pseudo *ping-pong* mechanism [1].

Vesicles, micelles and nanoparticles turned out to be a versatile and powerful tool to fabricate phosphodiesterases able to cleave the DNA model. On this regard a relevant example is provided by Konig et al. [167,168] The amphiphilic bimetallic Zn^{II} complex of cyclen **58b** exhibits noteworthy acceleration. It is significant to note the evident advantage of micellar system comparing its activity with that of the analogous complex **58a**-$(Zn^{II})_2$ lacking the C_{18} hydrophobic chain (entries 17 and 18, Table 2). The AuNPs **59**, saturated with stoichiometric amount of Zn^{II}, provide another noteworthy example of the use of a multivalent nanostructure able to efficiently cleave the phosphodiester (entry 19, Table 2) [169]. In the context of alternative materials as support for catalysis we can mention that the group of Guo reported the preparation of a double network hydrogel material bearing bis-amidoxime-Zn^{II} units as catalytic units in a polystyrene-polyethyleneimine polymer (see monomer **60**) [170]. This material shows a detectable reactivity toward phosphoesters including BNPP and represents the only example of a hydrogel-based phosphodiesterase. However, since there are not sufficient experimental details, it was impossible to extract quantitative data and to report them in Table 2.

In a recent article the study of the reactivity of the TACN units upon alkylation of nitrogen with different groups was reported [171]. This study highlights that the *N*-alkylation with R groups having intermediate bulkiness results in higher reactivity versus BNPP. In particular, complex **61**-Cu^{II}, having isopropyl groups on two N atoms, turned out to be the most reactive among those investigated [171].

8. Consideration about the use of effective molarity

Intramolecular reactions very often occur at significantly faster rates than their intermolecular counterparts. To quantify this enhanced reactivity, the effective molarity (EM) parameter has been employed [46]. The EM, defined as $EM = k_{intra}/k_{inter}$, represents the hypothetical concentration of one reactant required for an intermolecular reaction to proceed at the same rate as an intramolecular reaction. Broadly, EM can be interpreted as a measure of intramolecular reactivity, adjusted for the inherent reactivity of the end groups [176]. This allows for the comparison of reactivity data across different intramolecular reactions on a homogeneous scale. In many examples presented and discussed in thist work, essentially an intermolecular reaction is converted by the catalyst in an intramolecular one. According to the definition, the effective molarity can be given by Eq. (10), where the k_{cat} is the value of the first order rate constant as defined in Eq. (3) and k_{inter} is a second-order rate constant of the reaction of the substrate in the presence of two distinct molecules, each equipped with a single active unit. In contrast, in the reaction catalyzed by the supramolecular system, the two (or more) active functions operate intramolecularly.

$$EM = \frac{k_{cat}}{k_{inter}} \tag{10}$$

The EM parameter can be used to measure the efficiency of a catalytic scaffold, and it is extremely useful as it is independent on the concentration at which the experiments were carried out. The main issue is finding a suitable intermolecular reaction to measure the value of k_{intra}.

In the case the reaction of HPNP is catalyzed by the bare guanidine/ium dyad the k_{obs} for HPNP transesterification is given by Eq. (11), where G and GH^+ represent the guanidine and guanidinium, respectively [51].

$$k_{obs} = k_o + k_1[G] + k_2[G][GH^+] \tag{11}$$

k_o is attributable to the spontaneous reaction, k_1 to the general base catalysis of guanidine, and k_2 to the intermolecular effect of the guanidine/ium dyad. Therefore, the value of k_2 can be taken as k_{inter} in the determination of the effective molarity of catalytic systems based on this catalytic dyad (entries 63, 64, 76 and 77 of Table 1). In Table 3 are reported the EM values of these catalysts. The data provide a measurement of the degree of synergism displayed by the active functional units in the stabilization of the transition state of the reaction. These number are significantly higher than those for the closure of rings of comparable size, expected to be in the range of 10–50 mM [177].

Table 3
Effective molarity values (EMs) of the listed catalysts in the transesterification of HPNP.

Catalyst	EM (M)	Refs.
38	4.1	[53]
39	2.3	[51]
AuNPs **47**	4.7	[133]
NPs **48**	13.7	[139]

The EM values of the catalyst can thus serve as a measure of how effectively a scaffold—whether molecular or nanostructured—facilitates the cooperation of active functions, while also providing a quantitative estimate of the preorganization and flexibility of the spacers.

However, besides these very specific examples, the general use of EM in supramolecular catalysis, and even more in the enzymatic catalysis, is hampered by the limited availability of k_{cat} values and, above all, by the choice of a proper intermolecular reaction.

This is an essentially unresolvable problem. Indeed, the limited available information about the exact structure of the transition state of the intramolecular reaction, and of the stabilizing interactions involved in the catalyzed process, makes it extremely difficult to choose a proper and trustable intermolecular model reaction.

9. Conclusions

In conclusion, a comparison on equal terms of supramolecular catalysts by using simple models such as HPNP and BNPP reveals several key concepts. Catalysts based on metal ions, whether or not they include additional active units, generally demonstrate superior catalytic activity compared to systems that lack metal cations. The selection of the appropriate ligand-metal pair is critical for achieving high reaction rates and accelerations. It has also been shown that di- or multifunctional catalysts do not necessarily outperform monofunctional ones. Their efficiency is contingent upon the proper orientation and distance between functional groups, very difficult to predict a priori. Often when the active units are too close to one another, their effectiveness typically diminishes compared to a single active unit.

Moreover, the molecular platform utilized plays a crucial role in determining catalytic activity. The calix[4]arene platform, in particular, has been highlighted as an extremely versatile tool in enzyme model design, offering an excellent compromise between preorganization and flexibility. Catalysis involving cooperative action among three distinct functions remains a rarity when using conventional molecular platforms.

Nanostructured materials such as vesicles, micelles, nanoparticles, dendrimers, polymer brushes, and nanodiamonds present significant advantages by combining ease of preparation with high efficiency. These multifunctional systems can create adaptable catalytic sites where various active units can act cooperatively, thereby enhancing the overall catalytic performance. The use of such an adaptive approach definitely paves the way to the design and synthesis of novel catalytically active functional materials.

Declaration of competing interest

The authors declare that they have no known competing financial interests or personal relationships that could have appeared to influence the work reported in this paper.

Acknowledgments

This work was funded under the National Recovery and Resilience Plan (NRRP), Mission 4 Component 2 Investment 1.1 - Call for tender No. 104 of 02.02.2022 of Italian Ministry of University and Research funded by the European Union – NextGenerationEU, Award Number: Project code 2022285HC5, Concession Decree No. 1064 of 18.07.2023 adopted by the Italian Ministry of the University and Research, CUP D53D23010030006, SAMBA: Self-assembly of bacteria-targeting materials across the mesoscale. This work also benefited from the support of the COMP-R and X-Chem Initiatives, the "Departments of Excellence" program of the Italian Ministry for Education, University and Research (MUR 2023-2027).

Data availability

No data was used for the research described in the article.

References

[1] D. Voet, J.G. Voet, Biochemistry, 4th ed, John Wiley & Sons, Hoboken, NJ, 2011.
[2] R. Wolfenden, Degrees of difficulty of water-consuming reactions in the absence of enzymes, Chem. Rev. 106 (2006) 3379–3396.
[3] C.M. Cuchillo, M.V. Nogues, R.T. Raines, Bovine pancreatic ribonuclease: fifty years of the first enzymatic reaction mechanism, Biochemistry 50 (2011) 7835–7841.
[4] W. Yang, Nucleases: diversity of structure, function and mechanism, Q. Rev. Biophys. 44 (2011) 1–93.
[5] S.C. Walker, D.R. Engelke, Ribonuclease P: the evolution of an ancient RNA enzyme, Crit. Rev. Biochem. Mol. Biol. 41 (2006) 77–102.
[6] A.W. Nicholson, Ribonuclease III mechanisms of double-stranded RNA cleavage, Wiley Interdiscip. Rev. RNA 5 (2014) 31–48.
[7] D.H. Bechhofer, M.P. Deutscher, Bacterial ribonucleases and their roles in RNA metabolism, Crit. Rev. Biochem. Mol. Biol. 54 (2019) 242–300.
[8] R. Wolfenden, Benchmark reaction rates, the stability of biological molecules in water, and the evolution of catalytic power in enzymes, Annu. Rev. Biochem. 80 (2011) 645–667.
[9] G.K. Schroeder, C. Lad, P. Wyman, N.H. Williams, R. Wolfenden, The time required for water attack at the phosphorus atom of simple phosphodiesters and of DNA, PNAS 103 (2006) 4052–4055.
[10] R. Wolfenden, Primordial chemistry and enzyme evolution in a hot environment, Cell. Mol. Life Sci. 71 (2014) 2909–2915.
[11] J.G. Zalatan, D. Herschlag, Alkaline phosphatase mono- and Diesterase reactions: comparative transition state analysis, J. Am. Chem. Soc. 128 (2006) 1293–1303.
[12] M. Raynal, P. Ballester, A. Vidal-Ferran, P.W. van Leeuwen, Supramolecular catalysis. Part 2: artificial enzyme mimics, Chem. Soc. Rev. 43 (2014) 1734–1787.
[13] S. Mikkola, T. Lönnberg, H. Lönnberg, Phosphodiester models for cleavage of nucleic acids, Beilstein J. Org. Chem. 14 (2018) 803–837.
[14] J.R. Morrow, T.L. Amyest, J.P. Richard, Phosphate binding energy and catalysis by small and large molecules, Acc. Chem. Res. 41 (2008) 539–548.
[15] Z. Dong, Q. Luo, J. Liu, Artificial enzymes based on supramolecular scaffolds, Chem. Soc. Rev. 41 (2012) 7890–7908.
[16] M.D. Tomczyk, N. Kuźnik, K. Walczak, Cyclen-based artificial nucleases: three decades of development (1989–2022). part a – hydrolysis of phosphate esters, Coord. Chem. Rev. (2023) 481.
[17] Y. Aiba, J. Sumaoka, M. Komiyama, Artificial DNA cutters for DNA manipulation and genome engineering, Chem. Soc. Rev. 40 (2011) 5657–5668.
[18] D. Desbouis, I.P. Troitsky, M.J. Belousoff, L. Spiccia, B. Graham, Copper(II), zinc (II) and nickel(II) complexes as nuclease mimetics, Coord. Chem. Rev. 256 (2012) 897–937.
[19] C. Wende, C. Lüdtke, N. Kulak, Copper complexes of N-donor ligands as artificial nucleases, Eur. J. Inorg. Chem. 2014 (2014) 2597–2612.
[20] R. Salvio, The Guanidinium unit in the catalysis of phosphoryl transfer reactions: from molecular spacers to nanostructured supports, Chem. Eur. J. 21 (2015) 10960–10971.
[21] T. Joshi, B. Graham, L. Spiccia, Macrocyclic metal complexes for metalloenzyme mimicry and sensor development, Acc. Chem. Res. 48 (2015) 2366–2379.
[22] Z. Thompson, J.A. Cowan, Artificial metalloenzymes: recent developments and innovations in bioinorganic catalysis, Small 16 (2020) e2000392.
[23] B. Li, X. Xu, Y. Lv, Z. Wu, L. He, Y.F. Song, Polyoxometalates as potential artificial enzymes toward biological applications, Small 20 (2024) e2305539.
[24] F. Mancin, P. Scrimin, P. Tecilla, Progress in artificial metallonucleases, Chem. Commun. 48 (2012) 5545–5559.
[25] E. Kuah, S. Toh, J. Yee, Q. Ma, Z. Gao, Enzyme mimics: advances and applications, Chem. Eur. J. 22 (2016) 8404–8430.
[26] M.E. Gleave, B.P. Monia, Antisense therapy for cancer, Nat. Rev. Cancer 5 (2005) 468–479.
[27] A. Biroccio, C. Leonetti, G. Zupi, The future of antisense therapy: combination with anticancer treatments, Oncogene 22 (2003) 6579–6588.
[28] M. Anjomshoa, B. Amirheidari, Nuclease-like metalloscissors: biomimetic candidates for cancer and bacterial and viral infections therapy, Coord. Chem. Rev. 458 (2022).
[29] Z. Yu, J.A. Cowan, Metal complexes promoting catalytic cleavage of nucleic acids-biochemical tools and therapeutics, Curr. Opin. Chem. Biol. 43 (2018) 37–42.
[30] T.J.P. McGivern, S. Afsharpour, C.J. Marmion, Copper complexes as artificial DNA metallonucleases: from Sigman's reagent to next generation anti-cancer agent? Inorg. Chim. Acta 472 (2018) 12–39.
[31] B. Gyurcsik, A. Czene, Towards artificial metallonucleases for gene therapy: recent advances and new perspectives, Future Med. Chem. 3 (2011) 1935–1966.
[32] X. Ma, Y. Yin, Z. Geng, Z. Yang, J. Wen, Z. Wang, The first example of a model compound of RNase U2 and its intermediate with CPP directly monitored by ESI-MS, RSC Adv. 4 (2014) 50070–50073.
[33] T.K. Luong, G. Absillis, P. Shestakova, T.N. Parac-Vogt, Hydrolysis of the RNA model substrate catalyzed by a binuclear Zr(IV)-substituted Keggin polyoxometalate, Dalton Trans. 44 (2015) 15690–15696.
[34] G. Absillis, E. Cartuyvels, R.V. Deun, T.N. Parac-Vogt, Hydrolytic cleavage of an RNA-model phosphodiester catalyzed by a highly negatively charged Polyoxomolybdate $[Mo_7O_{24}]_6^-$ cluster, J. Am. Chem. Soc. 130 (2008) 17400–17408.
[35] N.S. Corby, G.W. Kenner, A.R. Todd, Studies on phosphorylation. Part X., The preparation of tetraesters of pyrophosphoric acid from diesters of phosphoric acid by means of exchange reactions, J. Chem. Soc. (1952) 1234–1243.
[36] D.M. Brown, D.A. Usher, J. Chem. Soc. (1965) 6558–6564.
[37] T. Koiket, E. Kimura, Roles of Zinc(I1) ion in phosphatases. A model study with Zinc(11)-macrocyclic polyamine complexes, J. Am. Chem. Soc. 113 (1991) 8935–8941.
[38] R. Breslow, Biomimetic chemistry and artificial enzymes catalysis by design, Acc. Chem. Res. 28 (1995) 146–153.
[39] J. Chin, M. Banaszczyk, V. Jubian, X. Zou, Co(III) complex promoted hydrolysis of phosphate Diesters: comparison in reactivity of rigid cfs-Diaquotetraazacobalt(III) complexes, J. Am. Chem. Soc. 111 (1989) 186–190.
[40] R. Cacciapaglia, A. Casnati, L. Mandolini, A. Peracchi, D.N. Reinhoudt, R. Salvio, A. Sartori, R. Ungaro, Efficient and selective cleavage of RNA oligonucleotides by calix[4]arene-based synthetic metallonucleases, J. Am. Chem. Soc. 129 (2007) 12512–12520.
[41] R. Salvio, S. Volpi, R. Cacciapaglia, A. Casnati, L. Mandolini, F. Sansone, Ribonuclease activity of an artificial catalyst that combines a ligated Cu(II) ion and a guanidinium group at the upper rim of a cone-calix[4]arene platform, J. Org. Chem. 80 (2015) 5887–5893.
[42] P.M. Scrimin, J. Czescik, S. Zamolo, T. Darbre, R. Rigo, C. Sissi, A. Pecina, L. Riccardi, M. De Vivo, F. Mancin, A gold nanoparticle Nanonuclease relying on a Zn(II) mononuclear complex, Angew. Chem. Int. Ed. 60 (2021) 1423–1432.
[43] L. Tjioe, A. Meininger, T. Joshi, L. Spiccia, B. Graham, Efficient plasmid DNA cleavage by copper(II) complexes of 1,4,7-triazacyclononane ligands featuring xylyl-linked guanidinium groups, Inorg. Chem. 50 (2011) 4327–4339.
[44] R. Salvio, R. Cacciapaglia, L. Mandolini, F. Sansone, A. Casnati, Diguanidinocalix [4]arenes as effective and selective catalysts of the cleavage of diribonucleoside monophosphates, RSC Adv. 4 (2014) 34412–34416.
[45] L. Lain, H. Lonnberg, T.A. Lonnberg, Buffer catalyzed cleavage of uridylyl-3′,5′-uridine in aqueous DMSO: comparison to its activated analog, 2-hydroxypropyl 4-nitrophenyl phosphate, Org. Biomol. Chem. 13 (2015) 3484–3492.
[46] E.V. Anslyn, D.A. Dougherty, Modern Physical Organic, Chemistry University Science Books, Sausalito California, 2006.
[47] H. Mayr, A.R. Ofial, The reactivity-selectivity principle: an imperishable myth in organic chemistry, Angew. Chem. Int. Ed. 45 (2006) 1844–1854.
[48] F.H. Zelder, R. Salvio, J. Rebek, A synthetic receptor for phosphocholine esters, Chem. Commun. (2006) 1280–1282.
[49] M. Zhao, L. Zhang, H.-Y. Chen, H.-L. Wang, L.-N. Ji, Z.-W. Mao, Effect of hydrophobic interaction cooperating with double Lewis acid activation in a zinc (ii) phosphodiesterase mimic, Chem. Commun. 46 (2010) 6497–6499.
[50] A.N. Nardi, A. Olivieri, M. D'Abramo, R. Salvio, Unveiling the cleavage mechanism of an RNA model compound on the whole pH scale: computations meet experiments in the determination of reaction rates, ChemPhysChem (2024) e202300873.
[51] L. Baldini, R. Cacciapaglia, A. Casnati, L. Mandolini, R. Salvio, F. Sansone, R. Ungaro, Upper rim Guanidinocalix[4]arenes as artificial phosphodiesterases, J. Org. Chem. 77 (2012) 3381–3389.
[52] R. Salvio, M. Moliterno, D. Caramelli, L. Pisciottani, A. Antenucci, M. D'Amico, M. Bella, Kinetic resolution of phosphoric diester by Cinchona alkaloid derivatives provided with a guanidinium unit, Cat. Sci. Technol. 6 (2016) 2280–2288.
[53] R. Salvio, L. Mandolini, C. Savelli, Guanidine-Guanidinium cooperation in bifunctional artificial phosphodiesterases based on Diphenylmethane spacers; gem-Dialkyl effect on catalytic efficiency, J. Org. Chem. 78 (2013) 7259–7263.
[54] J.K. Lassila, J.G. Zalatan, D. Herschlag, Biological phosphoryl-transfer reactions: understanding mechanism and catalysis, Annu. Rev. Biochem. 80 (2011) 669–702.

[55] L.F. Serafim, V.M. Jayasinghe-Arachchige, L. Wang, P. Rathee, J. Yang, N. S. Moorkkannur, R. Prabhakar, Distinct chemical factors in hydrolytic reactions catalyzed by metalloenzymes and metal complexes, Chem. Commun. 59 (2023) 8911–8928.
[56] C.M. Dupureur, One is enough: insights into the two-metal ion nuclease mechanism from global analysis and computational studies, Metallomics 2 (2010) 609–620.
[57] J.E. Murphy, B. Stec, L. Ma, E.R. Kantrowitz, Trapping and visualization of a covalent enzyme-phosphate intermediate, Nature 4 (1997) 618–622.
[58] A.J. Kirby, M. Medeiros, J.R. Mora, P.S.M. Oliveira, A. Amer, N.H. Williams, F. Nome, Intramolecular general base catalysis in the hydrolysis of a phosphate diester. Calculational guidance to a choice of mechanism, J. Org. Chem. 78 (2013) 1343–1353.
[59] G.E. Segreto, J. Alba, R. Salvio, M. D'Abramo, DNA cleavage by endonuclease I-DmoI: a QM/MM study and comparison with experimental data provide indications on the environmental effects, Theor. Chem. Accounts 139 (2020) 68.
[60] A.N. Nardi, A. Olivieri, A. Amadei, R. Salvio, M. D'Abramo, Modelling complex bimolecular reactions in a condensed phase: the case of phosphodiester hydrolysis, Molecules 28 (2023) 2152.
[61] J.E. Coleman, Structure and mechanism of alkaline phosphatases, Annu. Rev. Biophys. Biomol. Struct. 21 (1992) 441–483.
[62] J.G. Zalatan, T.D. Fenn, D. Herschlag, Comparative enzymology in the alkaline phosphatase superfamily to determine the catalytic role of an active-site metal ion, J. Mol. Biol. 384 (2008) 1174–1189.
[63] E.A. Galburt, B. Chevalier, W. Tang, M.S. Jurica, K.E. Flick, Raymond J. Monnat, B.L. Stoddard, A novel endonuclease mechanism directly visualized for I-PpoI, Nat. Struct. Biol. 6 (1999) 1096–1099.
[64] J.M. Thomas, J.-K. Yoon, D.M. Perrin, Investigation of the catalytic mechanism of a synthetic DNAzyme with protein-like functionality: an RNaseA mimic? J. Am. Chem. Soc. 131 (2009) 5648–5658.
[65] J.S.W. Tsang, A.A. Neverov, R.S. Brown, La^{3+}-catalyzed Methanolysis of Hydroxypropyl-p-nitrophenyl phosphate as a model for the RNA transesterification reaction, J. Am. Chem. Soc. 125 (2003) 1559–1566.
[66] P. Gomez-Tagle, I. Vargas-Zuniga, O. Taran, A.K. Yatsimirsky, Solvent effects and alkali metal ion catalysis in phosphodiester hydrolysis, J. Org. Chem. 71 (2006) 9713–9722.
[67] I. Sanchez-Lombardo, A.K. Yatsimirsky, Simplified speciation and improved phosphodiesterolytic activity of hydroxo complexes of trivalent lanthanides in aqueous DMSO, Inorg. Chem. 47 (2008) 2514–2525.
[68] B.K. Takasaki, J. Chin, Synergistic effect between lanthanum(III) and hydrogen peroxide in phosphate diester cleavage, J. Am. Chem. Soc. 115 (1993) 9337–9338.
[69] N.H. Williams, B. Takasaki, M. Wall, J. Chin, Structure and nuclease activity of simple Dinuclear metal complexes: quantitative dissection of the role of metal ions, Acc. Chem. Res. 32 (1999) 485–493.
[70] H. Daver, B. Das, E. Nordlander, F. Himo, Theoretical study of phosphodiester hydrolysis and transesterification catalyzed by an unsymmetric biomimetic dizinc complex, Inorg. Chem. 55 (2016) 1872–1882.
[71] C.I. Maxwell, N.J. Mosey, R. Stan Brown, DFT computational study of the methanolytic cleavage of DNA and RNA phosphodiester models promoted by the dinuclear Zn(II) complex of 1,3-bis(1,5,9-triazacyclododec-1-yl)propane, J. Am. Chem. Soc. 135 (2013) 17209–17222.
[72] C.A. Chang, T.-T. Wu, H.-Y. Lee, Hydrolysis and DFT structural studies of dinuclear Zn(II) and Cu(II) macrocyclic complexes of m-12N_3O-dimer and the effect of pH on their promoted HPNP hydrolysis rates, J. Coord. Chem. 69 (2016) 1388–1405.
[73] X. Zhang, X. Liu, D.L. Phillips, C. Zhao, Hydrolysis mechanisms of BNPP mediated by facial copper(ii) complexes bearing single alkyl guanidine pendants: cooperation between the metal centers and the guanidine pendants, Dalton Trans. 45 (2016) 1593–1603.
[74] R. Salvio, A. Casnati, Guanidinium promoted cleavage of phosphoric Diesters: kinetic investigations and calculations provide indications on the operating mechanism, J. Org. Chem. 82 (2017) 10461–10469.
[75] C.A. Chang, H.Y. Lee, S.L. Lin, C.N. Meng, T.T. Wu, Solution speciation, DFT calculations, luminescence properties and promoted Nitrophenyl-phosphate hydrolysis rates of Dinuclear lanthanide(III)-m-ODO2A-dimer macrocyclic complexes, Chem. Eur. J. 24 (2018) 6442–6457.
[76] R. Salvio, M. D'Abramo, Conformational mobility and efficiency in supramolecular catalysis. A computational approach to evaluate the performances of enzyme mimics, Eur. J. Org. Chem. (2020) 6004–6011.
[77] D. Wahnon, R.C. Hynes, J. Chin, Dramatic ligand effect in copper(II) complex promoted transesterification of a phosphate Diester, J. Chem. Soc. Chem. Commun. (1994) 1441–1442.
[78] M. Wall, R.C. Hynes, J. Chin, Double Lewis acid activation in phosphate Diester cleavage, Angew. Chem. Int. Ed. 32 (1993) 1633–1635.
[79] E. Kent Barefield, Coordination chemistry of N-tetraalkylated cyclam ligands—a status report, Coord. Chem. Rev. 254 (2010) 1607–1627.
[80] P. Lejault, K. Duskova, C. Bernhard, I.E. Valverde, A. Romieu, D. Monchaud, The scope of application of macrocyclic polyamines beyond metal chelation, Eur. J. Org. Chem. 2019 (2019) 6146–6157.
[81] R. Cacciapaglia, A. Casnati, L. Mandolini, D.N. Reinhoudt, R. Salvio, A. Sartori, R. Ungaro, Catalysis of diribonucleoside monophosphate cleavage by water soluble copper(II) complexes of calix[4]arene based nitrogen ligands, J. Am. Chem. Soc. 128 (2006) 12322–12330.
[82] P. Rossi, F. Felluga, P. Tecilla, F. Formaggio, M. Crisma, C. Toniolo, P. Scrimin, An azacrown-functionalized peptide as a metal ion based catalyst for the cleavage of a RNA-model substrate, Biopolymers 55 (2000) 496–501.
[83] P. Rossi, P. Tecilla, L. Baltzer, P. Scrimin, De Novo metallonucleases based on helix-loop-helix motifs, Chem. Eur. J. 10 (2004) 4163–4170.
[84] R. Cacciapaglia, A. Casnati, L. Mandolini, D.N. Reinhoudt, R. Salvio, A. Sartori, R. Ungaro, Di- and trinuclear Zn^{2+} complexes of calix[4]arene based ligands as catalysts of acyl and phosphoryl transfer reactions, J. Org. Chem. 70 (2005) 624–630.
[85] R. Cacciapaglia, A. Casnati, L. Mandolini, D.N. Reinhoudt, R. Salvio, A. Sartori, R. Ungaro, Calix[4]arene-based Zn^{2+} complexes as shape- and size-selective catalysts of ester cleavage, J. Org. Chem. 70 (2005) 5398–5402.
[86] T. Gunnlaugsson, R.J. Davies, M. Nieuwenhuyzen, C.S. Stevenson, R. Viguier, S. Mulready, Rapid hydrolytic cleavage of the mRNA model compound HPNP by glycine based macrocyclic lanthanide ribonuclease mimics, Chem. Commun. (2002) 2136–2137.
[87] M. Ruiz Kubli, A.K. Yatsimirsky, Phosphodiester cleavage by trivalent lanthanides in the presence of native cyclodextrins, Inorg. Chim. Acta 440 (2016) 9–15.
[88] T. Gunnlaugsson, M. Nieuwenhuyzen, C. Nolan, Synthesis, X-ray crystallographic, spectroscopic investigation and cleavage studies of HPNP by simple bispyridyl iron, copper, cobalt, nickel and zinc complexes as artificial nucleases, Polyhedron 22 (2003) 3231–3242.
[89] K. Worm, F.Y. Chu, K. Matsumoto, M.D. Best, V. Lynch, E.V. Anslyn, Preorganized bis-zinc phosphodiester cleavage catalysts possessing natural ligands: a lesson pertinent to bimetallic artificial enzymes, Chem. Eur. J. 9 (2003) 741–747.
[90] L. Bonfa, M. Gatos, F. Mancin, P. Tecilla, U. Toneliato, The ligand effect on the hydrolytic reactivity of Zn(II) complexes toward phosphate diesters, Inorg. Chem. 42 (2003) 3943–3949.
[91] F. Mancin, E. Rampazzo, P. Tecilla, U. Tonellato, Dinuclear metal complexes based on all-cis-2,4,6-triaminocyclohexane1,3,5-triol as catalysts for cleavage of phosphate esters, Eur. J. Org. Chem. 281-288 (2004).
[92] D. Bim, E. Svobodova, V. Eigner, L. Rulisek, J. Hodacova, Copper(II) and zinc(II) complexes of Conformationally constrained Polyazamacrocycles as efficient catalysts for RNA model substrate cleavage in aqueous solution at physiological pH, Chem. Eur. J. 22 (2016) 10426–10437.
[93] G. Zaupa, M. Martin, L.J. Prins, P. Scrimin, Determination of the activity of heterofunctionalized catalysts from mixtures, New J. Chem. 30 (2006) 1493–1497.
[94] X. Wu, H. Lin, J. Shao, H. Lin, Study on kinetics and mechanism of dinuclear metal zinc(II) complexes in promoting the hydrolysis of 2-hydroxy-propyl-p-nitrophenyl phosphate (HPNP), J. Mol. Catal. A Chem. 293 (2008) 79–85.
[95] X.-X. Wu, H.-K. Lin, H. Lin, Dinuclear Zn2+ metal complexes based on 1,10-phenanthroline derivates as catalysts for the hydrolysis of 2-hydroxypropyl-p-nitrophenyl phosphate (HPNP) and p-nitrophenyl phosphate (NPP), Transit. Met. Chem. 32 (2007) 1018–1024.
[96] T.K. Luong, T.T. Mihaylov, G. Absillis, P. Shestakova, K. Pierloot, T.N. Parac-Vogt, Phosphate Ester bond hydrolysis promoted by lanthanide-substituted Keggin-type Polyoxometalates studied by a combined experimental and density functional theory approach, Inorg. Chem. 55 (2016) 9898–9911.
[97] P. Molenveld, J.F.J. Engbersen, H. Kooijman, A.L. Spek, D.N. Reinhoudt, Efficient catalytic phosphate diester cleavage by the synergetic action of two Cu(II) centers in a dinuclear cis-diaqua Cu(II) calix[4]arene enzyme model, J. Am. Chem. Soc. 120 (1998) 6726–6737.
[98] R. Cacciapaglia, S. Di Stefano, L. Mandolini, R. Salvio, Reactivity of carbonyl and phosphoryl groups at calixarenes, Supramol. Chem. 25 (2013) 537–554.
[99] P. Molenveld, J.F.J. Engbersen, D.N. Reinhoudt, Synthesis of a dinuclear Zn-II-calix[4]arene enzyme model with additional general base groups - catalytic activity in phosphate diester transesterification, Eur. J. Org. Chem. (1999) 3269–3275.
[100] P. Molenveld, W.M.G. Stikvoort, H. Kooijman, A.L. Spek, J.F.J. Engbersen, D. N. Reinhoudt, Dinuclear and trinuclear Zn(II) calix[4]arene complexes as models for hydrolytic metallo-enzymes. Synthesis and catalytic activity in phosphate diester transesterification, J. Org. Chem. 64 (1999) 3896–3906.
[101] J. Czescik, Y. Lyu, S. Neuberg, P. Scrimin, F. Mancin, Host-guest allosteric control of an artificial phosphatase, J. Am. Chem. Soc. 142 (2020) 6837–6841.
[102] M. Diez-Castellnou, G. Salassa, F. Mancin, P. Scrimin, The Zn(II)-1,4,7-Trimethyl-1,4,7-Triazacyclononane complex: a monometallic catalyst active in two protonation states, Front. Chem. 7 (2019) 469.
[103] A. Scarso, U. Scheffer, M. Göbel, Q.B. Broxterman, B. Kaptein, F. Formaggio, C. Toniolo, P. Scrimin, A peptide template as an allosteric supramolecular catalyst for the cleavage of phosphate esters, PNAS 99 (2002) 5144–5149.
[104] N.J.V. Lindgren, J.R. Lars Geiger, C. Schmuck, L. Baltzer, Downsizing of enzymes by chemical methods: arginine mimics with low pKa values increase the rates of hydrolysis of RNA model compounds, Angew. Chem. Int. Ed. 48 (2009) 6722–6725.
[105] A. Scarso, G. Zaupa, F.B. Houillon, L.J. Prins, P. Scrimin, Tripodal, cooperative, and allosteric transphosphorylation metallocatalysts, J. Org. Chem. 72 (2007) 376–385.
[106] A.A. Neverov, Z.-L. Lu, C.I. Maxwell, M.F. Mohamed, C.J. White, J.S.W. Tsang, R. S. Brown, Combination of a Dinuclear Zn2+ complex and a medium effect exerts a 1012-fold rate enhancement of cleavage of an RNA and DNA model system, J. Am. Chem. Soc. 128 (2006) 16398–16405.
[107] S.E. Bunn, C.T. Liu, Z.-L. Lu, A.A. Neverov, R.S. Brown, The Dinuclear Zn(II) complex catalyzed cyclization of a series of 2-Hydroxypropyl aryl phosphate RNA models: progressive change in mechanism from rate-limiting P-O bond cleavage to substrate binding, J. Am. Chem. Soc. 129 (2007) 16238–16248.

[108] R.S. Brown, Z.-L. Lu, C.T. Liu, W.Y. Tsang, D.R. Edwards, A.A. Neverov, Dinuclear Zn(II) catalysts as biomimics of RNA and DNA phosphoryl transfer enzymes: changing the medium from water to alcohol provides enzyme-like rate enhancements, J. Phys. Org. Chem. 23 (2010) 1–15.
[109] M.F. Mohamed, R.S. Brown, Cleavage of an RNA model catalyzed by Dinuclear Zn (II) complexes containing rate-accelerating pendants. Comparison of the catalytic benefits of H-bonding and hydrophobic substituents, J. Org. Chem. 75 (2010) 8471–8477.
[110] J. Zan, H. Yan, Z.-F. Guo, Z.-L. Lu, Efficient syntheses of artificial nucleases containing mono-, di- and tri-[12]aneN3 ligating units through click chemistry, Inorg. Chem. Commun. 13 (2010) 1054–1056.
[111] Y. Luo, H. Lin, H. Lin, Kinetics and mechanism of promoted hydrolysis of 2-hydroxypropyl-p-nitrophenyl phosphate (HPNP) by complexes of RPAla and RPVal with La(III), Gd(III), J. Mol. Catal. A Chem. 263 (2007) 70–76.
[112] J.R. Morrow, O. Iranzo, Synthetic metallonucleases for RNA cleavage, Curr. Opin. Chem. Biol. 8 (2004) 192–200.
[113] O. Iranzo, A.Y. Kovalevsky, J.R. Morrow, J.P. Richard, Physical and kinetic analysis of the cooperative role of metal ions in catalysis of phosphodiester cleavage by a Dinuclear Zn(II) complex, J. Am. Chem. Soc. 125 (2003) 1988–1993.
[114] M.F. Mohamed, A.A. Neverov, R. Stan Brown, Investigation of the effect of oxy bridging groups in Dinuclear Zn(II) complexes that catalyze the cleavage of a simple phosphate Diester RNA analogue, Inorg. Chem. 48 (2009) 11425–11433.
[115] R. Bonomi, G. Saielli, U. Tonellato, P. Scrimin, F. Mancin, Insights on nuclease mechanism: the role of proximal ammonium group on phosphate esters cleavage, J. Am. Chem. Soc. 131 (2009) 11278–11279.
[116] P. Blondeau, M. Segura, R. Pérez-Fernández, J. de Mendoza, Molecular recognition of oxoanions based on guanidinium receptors, Chem. Soc. Rev. 36 (2007) 198–210.
[117] R. Salvio, R. Cacciapaglia, L. Mandolini, General base–guanidinium cooperation in bifunctional artificial phosphodiesterases, J. Org. Chem. 76 (2011) 5438–5443.
[118] J.R. Hiscock, M.R. Sambrook, P.B. Cranwell, P. Watts, J.C. Vincent, D.J. Xuereb, N.J. Wells, R. Raja, P.A. Gale, Tripodal molecules for the promotion of phosphoester hydrolysis, Chem. Commun. 50 (2014) 6217–6220.
[119] D.O. Corona-Martinez, O. Taran, A.K. Yatsimirsky, Mechanism of general acid-base catalysis in transesterification of an RNA model phosphodiester studied with strongly basic catalysts, Org. Biomol. Chem. 8 (2010) 873–880.
[120] K. Ariga, E.V. Anslyn, Manipulating the stoichiometry and strength of phosphodiester binding to a Bisguanidine cleft in Dmso water solutions, J. Org. Chem. 57 (1992) 417–420.
[121] D. Wirth-Hamdoune, S. Ullrich, U. Scheffer, T. Radanovic, G. Durner, M.W. Gobel, A Bis(guanidinium)alcohol attached to a hairpin polyamide: synthesis, DNA binding, and plasmid cleavage, ChemBioChem 17 (2016) 506–514.
[122] C. Gnaccarini, S. Peter, U. Scheffer, S. Vonhoff, S. Klussmann, M.W. Göbel, Site-specific cleavage of RNA by a metal-free artificial nuclease attached to antisense oligonucleotides, J. Am. Chem. Soc. 128 (2006) 8063–8067.
[123] R. Salvio, A. Casnati, L. Mandolini, F. Sansone, R. Ungaro, ATP cleavage by cone tetraguanidinocalix[4]arene, Org. Biomol. Chem. 10 (2012) 8941–8943.
[124] M.M. Kreevoy, E.H. Baughman, J. Phys. Chem. 78 (1974) 421–423.
[125] L. Tjioe, T. Joshi, C.M. Forsyth, B. Moubaraki, K.S. Murray, J. Brugger, B. Graham, L. Spiccia, Phosphodiester cleavage properties of copper(II) complexes of 1,4,7-triazacyclononane ligands bearing single alkyl guanidine pendants, Inorg. Chem. 51 (2012) 939–953.
[126] R. Salvio, S. Volpi, R. Cacciapaglia, F. Sansone, L. Mandolini, A. Casnati, Upper rim bifunctional cone-calix[4]arenes based on a ligated metal ion and a Guanidinium unit as DNAase and RNAase mimics, J. Org. Chem. 81 (2016) 4728–4735.
[127] C. Mahato, S. Menon, A. Singh, S.P. Afrose, J. Mondal, D. Das, Short peptide-based cross-beta amyloids exploit dual residues for phosphoesterase like activity, Chem. Sci. 13 (2022) 9225–9231.
[128] G. Zaupa, P. Scrimin, L.J. Prins, Origin of the dendritic effect in multivalent enzyme-like catalysts, J. Am. Chem. Soc. 130 (2008) 5699–5709.
[129] M. Martin, F. Manea, R. Fiammengo, L.J. Prins, L. Pasquato, P. Scrimin, Metallodendrimers as transphosphorylation catalysts, J. Am. Chem. Soc. 129 (2007) 6982–6983.
[130] G. Pieters, A. Cazzolaro, R. Bonomi, L.J. Prins, Self-assembly and selective exchange of oligoanions on the surface of monolayer protected au nanoparticles in water, Chem. Commun. 48 (2012) 1916–1918.
[131] R. Bonomi, A. Cazzolaro, A. Sansone, P. Scrimin, L.J. Prins, Detection of enzyme activity through catalytic signal amplification with functionalized gold nanoparticles, Angew. Chem. Int. Ed. 50 (2011) 2307–2312.
[132] R. Bonomi, A. Cazzolaro, L.J. Prins, Assessment of the morphology of mixed SAMs on au nanoparticles using a fluorescent probe, Chem. Commun. 47 (2011) 445.
[133] R. Salvio, A. Cincotti, Guanidine-based self-assembled monolayers on au nanoparticles as artificial phosphodiesterases, RSC Adv. 4 (2014) 28678–28682.
[134] J. Czescik, S. Zamolo, T. Darbre, R. Rigo, C. Sissi, A. Pecina, L. Riccardi, M. De Vivo, F. Mancin, P. Scrimin, A gold nanoparticle Nanonuclease relying on a Zn(II) mononuclear complex, Angew. Chem. Int. Ed. 60 (2021) 1423–1432.
[135] J. Czescik, S. Zamolo, T. Darbre, F. Mancin, P. Scrimin, Factors influencing the activity of Nanozymes in the cleavage of an RNA model substrate, Molecules 24 (2019).
[136] C. Pezzato, J.L. Chen, P. Galzerano, M. Salvi, L.J. Prins, Catalytic signal amplification for the discrimination of ATP and ADP using functionalised gold nanoparticles, Org. Biomol. Chem. 14 (2016) 6811–6820.
[137] C. Wang, H. Zhao, Polymer brushes and surface nanostructures: molecular design, precise synthesis, and self-assembly, Langmuir 40 (2024) 2439–2464.
[138] A. Murad Bhayo, Y. Yang, X. He, Polymer brushes: synthesis, characterization, properties and applications, Prog. Mater. Sci. 130 (2022) 101000.
[139] C. Savelli, R. Salvio, Guanidine-based polymer brushes grafted onto silica nanoparticles as efficient artificial phosphodiesterases, Chem. Eur. J. 21 (2015) 5856–5863.
[140] L. Gabrielli, L.J. Prins, F. Rastrelli, F. Mancin, P.M. Scrimin, Hydrolytic nanozymes, Eur. J. Org. Chem. (2020) 5044–5055.
[141] F. Mancin, P. Scrimin, P. Tecilla, U. Tonellato, Amphiphilic metalloaggregates: catalysis, transport, and sensing, Coord. Chem. Rev. 253 (2009) 2150–2165.
[142] D. Lisi, C.A. Vezzoni, A. Casnati, F. Sansone, R. Salvio, Intra- and intermolecular cooperativity in the catalytic activity of phosphodiester cleavage by self-assembled systems based on Guanidinylated calix[4]arenes, Chem. Eur. J. 29 (2023) e202203213.
[143] P. Solis Munana, G. Ragazzon, J. Dupont, C.Z. Ren, L.J. Prins, J.L. Chen, Substrate-induced self-assembly of cooperative catalysts, Angew. Chem. Int. Ed. 57 (2018) 16469–16474.
[144] C.Z.J. Ren, P. Solís-Muñana, G.G. Warr, J.L.Y. Chen, Dynamic and modular formation of a synergistic transphosphorylation catalyst, ACS Catal. 10 (2020) 8395–8401.
[145] M. Poznik, U. Maitra, B. Konig, The interface makes a difference: lanthanide ion coated vesicles hydrolyze phosphodiesters, Org. Biomol. Chem. 13 (2015) 9789–9792.
[146] Priyanka, S. Kaur Brar, S. Maiti, Analyzing catalytic co-operativity and membrane parameters in a substrate-driven vesicular assembly modified by nucleotides, ChemNanoMat 8 (2022) e202100498.
[147] N. Liu, P. Gao, H.Y. Lu, L. Fang, J. Nicolas, T. Ha-Duong, J.S. Shen, Polyfluoroalkyl chain-based assemblies for biomimetic catalysis, Chem. Eur. J. 30 (2024) e202302669.
[148] V.N. Mochalin, O. Shenderova, D. Ho, Y. Gogotsi, The properties and applications of nanodiamonds, Nat. Nanotechnol. 7 (2011) 11–23.
[149] Y. Zhang, K.Y. Rhee, D. Hui, S.-J. Park, A critical review of nanodiamond based nanocomposites: synthesis, properties and applications, Compos. B: Eng. 143 (2018) 19–27.
[150] K. Turcheniuk, V.N. Mochalin, Biomedical applications of nanodiamond, Nanotechnology 28 (2017) 252001.
[151] A.M. Schrand, H. Huang, C. Carlson, J.J. Schlager, E. Osawa, S.M. Hussain, L. Dai, Are diamond nanoparticles cytotoxic? J. Phys. Chem. B 111 (2007) 2–7.
[152] Y. Lin, X. Sun, D.S. Su, G. Centi, S. Perathoner, Catalysis by hybrid sp(2)/sp(3) nanodiamonds and their role in the design of advanced nanocarbon materials, Chem. Soc. Rev. 47 (2018) 8438–8473.
[153] A.V. Sinolits, M.G. Chernysheva, A.G. Popov, A.V. Egorov, G.A. Badun, Hyaluronic acid adsorption on nanodiamonds: quantitative characteristics and mechanism, Colloids Surf. A Physicochem. Eng. Asp. (2021) 618.
[154] C.A. Vezzoni, A. Casnati, S. Orlanducci, F. Sansone, R. Salvio, Enzyme mimics based on Guanidinocalix[4]arene/ Nanodiamond hybrid systems with phosphodiesterase activity, ChemCatChem (2024) e202301477.
[155] A.M. Fanning, S.E. Plush, T. Gunnlaugsson, Tri- and tetra-substituted cyclen based lanthanide(III) ion complexes as ribonuclease mimics: a study into the effect of log Ka, hydration and hydrophobicity on phosphodiester hydrolysis of the RNA-model 2-hydroxypropyl-4-nitrophenyl phosphate (HPNP), Org. Biomol. Chem. 13 (2015) 5804–5816.
[156] M. Livieri, F. Mancin, G. Saielli, J. Chin, U. Tonellato, Mimicking enzymes: cooperation between organic functional groups and metal ions in the cleavage of phosphate diesters, Chem. Eur. J. 13 (2007) 2246–2256.
[157] S. Albedyhl, D. Schnieders, A. Jancsó, T. Gajda, B. Krebs, Heterodinuclear zinc (II)−iron(III) complexes and dinuclear zinc complexes as models for zinc-containing phosphatases, Eur. J. Inorg. Chem. (2002) 1400–1409.
[158] T. Gajda, A. Jancsó, S. Mikkola, H. Lönnberg, H. Sirges, Crystal structure, solution properties and hydrolytic activity of an alkoxo-bridged dinuclear copper(ii) complex, as a ribonuclease model, J. Chem. Soc. Dalton Trans. 8 (2002) 1757–1763.
[159] R. Salvio, S. Volpi, T. Folcarelli, A. Casnati, R. Cacciapaglia, A calix[4]arene with acylguanidine units as an efficient catalyst for phosphodiester bond cleavage in RNA and DNA model compounds, Org. Biomol. Chem. 17 (2019) 7482–7492.
[160] O. Taran, A.K. Yatsimirsky, Phosphodiesterolytic activity of alkaline-earth cations in aqueous DMSO, Chem. Commun. (2004) 1228–1229.
[161] O. Taran, F. Medrano, A.K. Yatsimirsky, Rapid hydrolysis of model phosphate diesters by alkaline-earth cations in aqueous DMSO: speciation and kinetics, Dalton Trans. (2008) 6609–6618.
[162] C.A. Chang, Y.-P. Chen, C.-H. Hsiao, Kinetics of Bis(p-nitrophenyl)phosphate (BNPP) hydrolysis reactions with trivalent lanthanide complexes ofN-Hydroxyethyl(ethylenediamine)-N,N′,N′-triacetate (HEDTA), Eur. J. Inorg. Chem. 2009 (2009) 1036–1042.
[163] M. Arca, A. Bencini, E. Berni, C. Caltagirone, F.A. Devillanova, F. Isaia, A. Garau, C. Giorgi, V. Lippolis, A. Perra, L. Tei, B. Valtancoli, Coordination properties of new bis(1,4,7-triazacyclononane) ligands: a highly active dizinc complex in phosphate diester hydrolysis, Inorg. Chem. 42 (2003) 6929–6939.
[164] M. Livieri, F. Mancin, U. Tonellato, J. Chin, Multiple functional group cooperation in phosphate diester cleavage promoted by Zn(II) complexes, Chem. Commun. (2004) 2862–2863.
[165] R. Salvio, S. Volpi, R. Cacciapaglia, F. Sansone, L. Mandolini, A. Casnati, Phosphoryl transfer processes promoted by a trifunctional calix[4]arene inspired by DNA topoisomerase I, J. Org. Chem. 81 (2016) 9012–9019.
[166] M.R. Redinbo, L. Stewart, P. Kuhn, J.J. Champoux, W.G.J. Hol, Crystal structures of human topoisomerase I in covalent and noncovalent complexes with DNA, Science 279 (1998) 1504–1513.

[167] B. Gruber, E. Kataev, J. Aschenbrenner, S. Stadlbauer, B. Konig, Vesicles and micelles from amphiphilic zinc(II)-cyclen complexes as highly potent promoters of hydrolytic DNA cleavage, J. Am. Chem. Soc. 133 (2011) 20704–20707.
[168] M. Subat, K. Woinaroschy, C. Gerstl, B. Sarkar, W. Kaim, B. Konig, 1,4,7,10-tetraazacyclododecane metal complexes as potent promoters of phosphodiester hydrolysis under physiological conditions, Inorg. Chem. 47 (2008) 4661–4668.
[169] R. Bonomi, F. Selvestrel, V. Lombardo, C. Sissi, S. Polizzi, F. Mancin, U. Tonellato, P. Scrimin, Phosphate diester and dna hydrolysis by a multivalent, nanoparticle-based catalyst, J. Am. Chem. Soc. 130 (2008) 15744–15745.
[170] L. Wang, P. Jiang, W. Liu, J. Li, Z. Chen, T. Guo, Molecularly imprinted self-buffering double network hydrogel containing bi-amidoxime functional groups for the rapid hydrolysis of organophosphates, J. Hazard. Mater. 444 (2023) 130332.
[171] M. Buzikova, R. Willimetz, J. Kotek, The hydrolytic activity of copper(II) complexes with 1,4,7-Triazacyclononane derivatives for the hydrolysis of phosphate Diesters, Molecules 28 (2023) 7542.
[172] F.H. Fry, A.J. Fischmann, M.J. Belousoff, L. Spiccia, J. Brügger, Kinetics and mechanism of hydrolysis of a model phosphate Diester by $[Cu(Me_3tacn)(OH_2)_2]^{2+}$ (Me_3tacn = 1,4,7-Trimethyl-1,4,7-triazacyclononane), Inorg. Chem. 44 (2005) 941–950.
[173] C. Bazzicalupi, A. Bencini, E. Berni, A. Bianchi, P. Fornasari, C. Giorgi, B. Valtancoli, Zn(II) coordination to polyamine macrocycles containing dipyridine units. New insights into the activity of dinuclear Zn(II) complexes in phosphate ester hydrolysis, Inorg. Chem. 43 (2004) 6255–6265.
[174] M. Grossenbacher, W. Foley, G.T. Musie, Tetranuclear iron(III) complexes with a carboxylate-rich ligand as synthetic mimics of phosphoesterases in aqueous media, Inorg. Chim. Acta 543 (2022) 121195.
[175] L. Tjioe, A. Meininger, T. Joshi, L. Spiccia, B. Graham, Efficient plasmid DNA cleavage by copper(II) complexes of 1,4,7-triazacyclononane ligands featuring xylyl-linked guanidinium groups, Inorg. Chem. 50 (2011) 4327–4339.
[176] S. Di Stefano, R. Cacciapaglia, L. Mandolini, Supramolecular control of reactivity and catalysis - effective molarities of recognition-mediated bimolecular reactions, Eur. J. Org. Chem. 2014 (2014) 7304–7315.
[177] C. Galli, L. Mandolini, The role of ring strain on the ease of ring closure of bifunctional chain molecules, Eur. J. Org. Chem. (2000) 3117–3125.

Alessandro Casnati obtained his PhD in 1991 from the University of Parma under the supervision of Prof. Rocco Ungaro. In 1990 he spent a research period at the Twente University, The Netherlands, in the laboratory of Prof. David N. Reinhoudt. In 1994 he started his independent career and in 1998 and he was appointed associate professor of Organic Chemistry. He is recipient of the "G. Ciamician" (1997) and "A. Mangini" (2019) medals, both awarded by the Division of Organic Chemistry of the Italian Chemical Society. Since 2015 he is full professor of Organic Chemistry at Parma University. His research interests are in the field of supramolecular chemistry, supramolecular catalysis and bioorganic chemistry.

Riccardo Salvio received his PhD in 2005 from University of Rome La Sapienza (Italy) under the supervision of Prof. Luigi Mandolini. After his PhD, he moved to the USA where he spent the years 2005–2007 as a Research Associate in the group of Prof. Julius Rebek Jr. at The Scripps Research Institute in La Jolla, California. Then he moved to The Netherlands, joining the group of Prof. David N. Reinhoudt as a Postdoc, at the University of Twente and in 2009 he has started his independent career at La Sapienza University. In 2019 he moved to Tor Vergata University and in 2022 he was appointed associate professor in the same institution. His research interests include homogeneous catalysis, supramolecular chemistry, and physical organic chemistry.